Elastostatic assessment of several mixed/displacement-based laminated plate theories, differently accounting for transverse normal deformability

Ugo Icardi, Andrea Urraci

Politecnico di Torino, Italy

A R T I C L E I N F O

A B S T R A C T

Several multilayered physically-based plate theories are derived under different limiting assumptions on displacement, strain and stress fields, either in displacement-based or mixed Hu-Washizu and Helinger-Reissner form, and assuming different layerwise functions. Their features are reminiscent to those of theories published in the literature, or are entirely new. The present study aims to evaluate how different forms of description of the transverse normal deformation and stress affect accuracy. At the same time, the purpose is also to see if a much broader degree of generalization of what characterizing currently available physically-based zig-zag theories can be achieved through a redefinition of coefficients obtained by imposing the fulfillment of physical constraints, namely interfacial stress compatibility and local equilibrium equations across the thickness through use of symbolic calculus tool. Besides calculating exactly quantities, this tool enables users to choose representation form and zig-zag functions as desired, keeping fixed the d.o.f. to five. Challenging benchmarks with strong layerwise effects are considered, for which an accurate description of the transverse normal deformation effect is important. They include distributed/localized step loading and different boundary conditions. Effects of constraint stresses at supports are accounted for. Numerical results show that whenever the whole set of physical constraints is enforced across the thickness to redefine coefficients, the choice of the representation form and of zig-zag functions is immaterial and more importantly, accurate results are obtained with few variables and a low expansion order of solutions. Otherwise results are sensitive to the choices made.

© 2019 Elsevier Masson SAS. All rights reserved.

1. Introduction

Laminated and sandwich composites are key materials in many engineering fields, by virtue of their excellent specific strength and stiffness, fatigue and energy absorption properties, better resistance to corrosion and greater design flexibility. In particular, they allow to get higher speed, longer range, larger payloads, a reduction of pollution and better operating economy.

However, sophisticated theoretical and computational structural models are required to ward off any possible catastrophic failure or intolerable loss of performance in service of structures made of them, which typically exhibit three-dimensional stress fields and complex failure mechanisms. Unlike non-layered materials, their displacement field must be C°-continuous (zig-zag effect) so to ensure the continuity of out-of-plane stresses and then equilibrium.

So far, many multi-layered plate theories have been proposed, which can be categorized into equivalent single-layer (ESL), discrete-layer (DL) and zig-zag (ZZ) theories (acronyms are explained in Table 1). A comprehensive review and extensive discussion are presented in the book by Reddy [1] and in the papers [2–13]. Theories further subdivide into displacement-based or mixed formulations because displacements, as strains and stress fields can be chosen separately from one another.

The merit of ZZ, is to strike the right balance between accuracy and cost saving, allowing designers' demand of theories in a simple already accurate form to be met. They can be distinguished into physically-based/Di Sciuva's like [14] (DZZ) or kinematic-based/Murakami's like [15] (MZZ) zig-zag theories. A comprehensive discussion of MZZ, which today are the most used, along with extensive applications are given by Carrera [7–9], Carrera and coworkers [16,17], Demasi [10,11] and Rodrigues et al. [18]. They assume zig-zag functions a

Table 1
Acronyms, abbreviations and appellations of theories. New theories of this paper are indicated in bold.

Symbol	Explanation	Symbol	Explanation
CUF	Carrera's unified formulation [7]	**MHRO**	Variant of MHR with an additional d.o.f. $u_{\alpha,\beta}^{(3)}$, $u_\varsigma^{(4)}$ (sect. 3.1).
DL	Discrete layer theories	MHR4	Refined variant of MHR #1 $u_{\alpha,\beta}^{(3)}$, $u_\varsigma^{(4)}$ (sect. 3.2, Ref. [24]).
DZZ	Physically-based zig-zag theories	MHR4±	MHR4 with zig-zag function sign determined on a physical basis (sect. 3.2, Ref. [29]).
ESL	Equivalent single layer theories	MHWZZA	Modified HWZZ theory $u_{\alpha,\beta}^{(3)}$, $u_\varsigma^{(4)}$ (sect. 3.2, Ref. [24]).
FEA 3-D	Mixed solid 3-D elements (Ref. [50]).	MHWZZA4	Modified MHWZZA theory $u_{\alpha,\beta}^{(3)}$, $u_\varsigma^{(4)}$ (sect. 3.2, Ref. [24]).
HLT	Hierarchical theories [22], [23]	MZZ	Kinematic-based zig-zag theories
HR	Hellinger-Reissner variational theorem	RZT	Refined zig-zag theory (Ref. [41]).
HRZZ	Mixed HR theory with uniform transverse displacement $u_{\alpha,\beta}^{(3)}$, $u_\varsigma^{(0)}$ sect. 3.3	ZZ	Zig-zag theories
HRZZ4	Mixed HR theory with fourth-order transverse displacement $u_{\alpha,\beta}^{(3)}$, $u_\varsigma^{(4)}$ sect. 3.3	ZZ_NA1	Not adaptive DZZ $u_{\alpha,\beta}^{(3)}$, $u_\varsigma^{(4)}$ (sect. 2.4.1, Ref. [19]).
HW	Hu-Washizu variational theorem	**ZZ_NA2**	Variant of ZZ_NA1 with different representation across the thickness (sect. 2.4.1).
HWZZ	HW zig-zag mixed theory $u_{\alpha,\beta}^{(3)}$, $u_\varsigma^{(4)}$ (sect. 2.5, Ref. [24]).	ZZA	Zig-zag adaptive theory $u_{\alpha,\beta}^{(3)}$, $u_\varsigma^{(4)}$ (sect. 2.4, Ref. [26]).
HWZZM	Mixed Hu-Washizu zig-zag theory with Murakami's like zig-zag functions, $u_{\alpha,\beta}^{(3)}$, $u_\varsigma^{(4)}$ (sect. 2.6, Ref. [29]).	**ZZA1**	Modified ZZA theory #1 (sect. 2.4.1).
HWZZM(□)	Variants of HWZZM, type □ (sect. 2.6.1, Ref. [29]).	**ZZA2**	Modified ZZA theory #2 (sect. 2.4.1).
MHR	MZZ cubic-quartic mixed HR theory $u_{\alpha,\beta}^{(3)}$, $u_\varsigma^{(4)}$ (sect. 3.1, Ref. [24]).	**ZZA3**	Modified ZZA theory #3 (sect. 2.4.1).
MHR±	MHR with zig-zag function sign determined on a physical basis (sect. 3.1, Ref. [29]).	♠	ZZA, ZZA1, ZZA2, ZZA3, HWZZ, HWZZM, giving accurate coincident results reported in Tables and Figures.
		□ = A, B, B2, C, C2, 0 (variants of theory)	

priori featuring a periodic change of the slope of displacements at interfaces, therefore don't care of orientation angle, material properties and thickness of constituent layers. Their stress fields are assumed apart within the framework of Hellinger-Reissner variational theorem (HR), as a consequence C° formulations suitable for development of finite elements are easily obtainable. Carrera's unified formulation (CUF) [7], which allows displacements to take arbitrary forms that can be chosen by the user as an input of the analysis, is able to get existing and arbitrary mixed, MZZ and ESL structural models as particularizations. DZZ incorporate layerwise contributions as the product of linear [14] or nonlinear [19] zig-zag functions and unknown zig-zag amplitudes, which are determined by enforcing the fulfillment of stress continuity conditions at layer interfaces. In short, they enrich the coarse representation of ESL through layerwise contributions without increasing the number of unknowns. DZZ based on a global-local superposition of displacement fields proposed by Li and Liu [20] and refined over the years by Zhen and Wanji [21] have coefficients of local groups determined by enforcing displacement and stress constraints without including explicitly zig-zag functions.

Hierarchical theories (HLT) been developed within the framework of CUF to achieve greater numerical efficiency by Catapano et al. [22] and de Miguel et al. [23], which also do not explicitly contain zig-zag functions. In these theories, a hierarchical set of locally defined polynomials ensuring the C°-continuous requirement is assumed. To mitigate the interfacial stress jumps, direct consequence of the omission of zig-zag functions, a high degree of expansion of variables is required, which turns out into a high number of unknowns.

Also DL suffer from an excessive number of unknowns, their variables being assumed for each individual constituent layer. Consequently, they could overwhelm the computational capacity when structures of industrial interest are analyzed. ESL are computationally efficient, but since they disregard the zig-zag effect they cannot provide accurate stress predictions.

Examining the results of MZZ and DZZ available in the literature and of [24], it could be noticed that the former do not very accurately predict through-thickness displacement fields, although they use many d.o.f. for each displacement (15 in Brischetto et al. [25]), while they accurately predict stresses. On the contrary, DZZ developed as a generalization of ZZA theory [26], whose coefficients are redefined across the thickness through the enforcement of stress compatibility and equilibrium (hence their appellative adaptive), accurately predicts both fields with just five d.o.f. Recent studies by Gherlone [27] and Groh and Weaver [28], as well as those in [24] and [29] also show that MZZ are less accurate than DZZ with the same degree of representation, while Zhen and Wanji's [30] show that most sophisticated MZZ are accurate. From all this, it appears that DZZ are more accurate than MZZ with a low expansion order, but as the expansion order increases, the latter become accurate anyway.

As DZZ can obtain the due accuracy with a low computational burden, it follows the utility of the studies that aim at increasing their degree of generality and flexibility of use. In this context it is also important their assessment for cases whose strong layerwise effect makes modeling demanding.

So far, power series expansion, hierarchic polynomials, Taylor's series, trigonometric and exponential functions, a combination of both, radial basis functions (see [18,31–37]) and Hermite splines [38,39] have been used to represent variables across the thickness, in order to find the most efficient formulation. However, the authors in [29] have preliminarily shown that different theories lead to the same result if displacement field coefficients and zig-zag amplitudes are determined in exact form by enforcing the same whole set of constraint conditions via symbolic calculus. Indeed, symbolic calculus always determines the same exact result compensating for the mutation of functions. On the contrary, theories with only a partial fulfillment of constraints highlights a strong sensitivity of results from the assumptions made like for studies [18] and [31–39]. It is worth remembering that in this form symbolic calculus turns out to be an automatic tool enabling users to freely choose the type of representation and the zig-zag functions as desired.

Mixed formulations represent a viable option to keep kinematics simple and simultaneously obtain accurate predictions without having to incorporate a piecewise transverse displacement to account for the transverse normal deformability effect, as shown e.g., by the HW theory by Zhen and Wanji [30], HR theories by Kim and Cho [40], Tessler et al. [41], Barut et al. [42] and Iurlaro et al. [43].

However, given the importance of the transverse normal deformability effect (see, e.g. Icardi [19], Icardi and Sola [26], Shariyat [44], Carrera and Ciuffreda [45], Rekatsinas et al. [46] and Mattei and Bardella [47]), and the only partial accuracy of mixed models with simplified kinematics, as evidenced in [24] and [29], it seems that such mixed models can be used only for analysis of cases wherein the transverse normal deformation can just be described approximately. Such cases comprise the prediction of static response quantities under global distributed loading, uniform plate geometry and a slight variation of the elastic properties of layers. On the contrary, studies of high-frequency vibrations, transient response analyzes, localized loading, geometric and non-uniformity of properties require a very accurate description of the transverse normal deformability.

In light of the above considerations, boundary conditions, loadings and lay-ups giving rise to stronger layerwise effects from those used in the past are required to thoroughly test theories. Clamped edges are particularly interesting [17,41] since kinematic variables should vanish without incorrectly resulting into a vanishing transverse shear force resultant, as erroneously predicted by traditional plate models.

It becomes important from the previous discussion to clarify whether adaptive DZZ, like those of [24] and [29], can really provide an equivalent degree of generality as MZZ, hierarchical axiomatic/asymptotic theories and CUF under strong layerwise effects. It also becomes important to verify whether the potential advantage of DZZ of requiring a low expansion order of variables and few d.o.f. for being accurate occurs in practice. Moreover, it is important to check on a wide range of applications if indeed DZZ are adaptable case by case, given that the choice of their zig-zag and representation functions can be arbitrary, as preliminarily observed for the benchmarks considered in [29] and [48].

In light of the previous discussion, the intended aim of this paper is to thoroughly show by numerical assessments that adaptive theories [24,29,48] and new ones developed in this paper as their generalizations or mutations, (i) can allow an arbitrary choice of the displacement field and of zig-zag functions without the result changing, (ii) whenever physical constraints are satisfied in a point-wise sense across the thickness through the redefinition of coefficients.

In order to prove this, zig-zag functions that are arbitrarily chosen in a different way one from the other and representation functions that differ for each displacement and from region to region across the thickness are considered. Also variants wherein zig-zag functions are omitted, their role being played by coefficients redefined across the thickness, are considered. Lower-order theories, whose features are reminiscent to ones published in the literature, are considered for sake of comparison. For these and for the theories that only partially enforce the set of constraints the aim is to prove that the solution loses accuracy and becomes strongly dependent on the choices made.

A further purpose of this study is also to demonstrate that adaptive theories can reach a degree of generality and flexibility of use similar to that of axiomatic/asymptotic theories and CUF, requiring a much lower number of unknowns to get the same accuracy even for challenging cases with strong layerwise effects.

Challenging benchmarks retaken from the literature or new are used to test the accuracy of theories (Table 2 provides a quick reference pattern of all cases considered in the paper). Whenever available, exact solutions are considered as reference solutions, otherwise FEA 3-D is used.

2. Laminated plate theories of this paper

Hereafter the theoretical framework of structural models is discussed starting from basic notations and assumptions, then how closed-form solutions are obtained and the specific features of each theory are examined. However, to limit the length of the paper, just displacements, strain and stress fields are discussed into details since governing equations can be derived in a in a straightforward way from variational theorems.

2.1. Notations

The study is restricted to laminated plates subject to small deformations. Cell-scale effects of honeycomb core being disregarded, sandwiches are described as multi-layered structures. As usual for this type of study, constituent layers are assumed to have a uniform thickness h^k, linear elastic orthotropic properties and are perfectly bonded to each other and bonding interlayer film is disregarded.

A rectangular, right-handed Cartesian coordinate reference system $(\alpha, \beta, \varsigma)$ is assumed as reference frame on the middle reference plane Ω, (α, β) being assumed as the in-plane coordinates and therefore ς as the thickness coordinate ($\varsigma \in [-h/2; h/2]$, h being the overall thickness). The position of the upper and lower surfaces of the generic layer k are denoted by $^{(k)}\varsigma^+$ and $^{(k)}\varsigma^-$, respectively, while ς_k represents the coordinate of layer interfaces. L_α and L_β symbolize the plate side-length in the α- and β-directions. Subscripts $_k$ and superscripts ^{k} indicate that a quantity belongs to the layer k, while ^{u} and $_l$ mark the properties at upper and lower faces of the laminate. Elastic in-plane and transverse displacement components are indicated as u_α and u_ς, while in-plane and out-of-plane strain and stress components are indicated respectively as ε_{ij}, $\varepsilon_{\alpha\varsigma}$, $\varepsilon_{\varsigma\varsigma}$ and σ_{ij}, $\sigma_{\alpha\varsigma}$, $\sigma_{\varsigma\varsigma}$ ($\gamma_{\alpha\beta} = 2\varepsilon_{\alpha\beta}$).

To distinguish their origin, strains are further specified as $\varepsilon_{ij}^u = 1/2(u_{i,j} + u_{j,i})$ and $\varepsilon_{ij}^\sigma = (E_{ijkl})^{-1}\sigma_{kl}$, respectively if they come from kinematic $[.]^u$ or stress-strain $[.]^\sigma$ relations $\sigma_{ij}^\varepsilon = E_{ijkl}\varepsilon_{kl}$, being $C_{ijkl} = (E_{ijkl})^{-1}$.
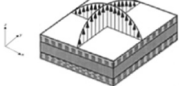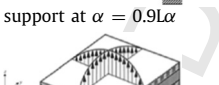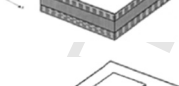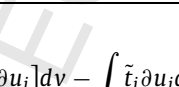
Einstein summation convention is used throughout the paper and a comma is used to indicate spatial derivatives, e.g. $(.)_{,\alpha} = \partial(.)/\partial\alpha, (.)_{,\varsigma} = \partial(.)/\partial\varsigma$. As usual, the prismatic plate volume V is assumed to be bounded by a surface S that is split into a surface S_t on which surface tractions are prescribed and a surface S_u on which surface displacements are prescribed. Body forces b_i on V, prescribed surface tractions $\tilde{t}_i$ on S_t and prescribed displacements $\tilde{u}_i$ on S_u are assumed to act.

2.2. Brief reminder of variational theorems used in this study

Theories wherein displacements, strains and stresses are assumed as primary variables are developed using a generalized version HW^g of Hu-Washizu canonical functional whose primary displacement boundary condition link is weakened as $\int_{S_u}(u_i - \tilde{u}_i)n_j\partial\sigma_{ij}dS = 0$ (i, j coincide in turn with α, β or ς) and which generates the following variational statement:

Table 2
Data of cases.

Case	Lay-up	Layer thickness	Material	Sketch	Loading	Lα/h	Lβ/Lx
a$^{(*§)}$	$[0/90/0/0/0/90]_S$	$[((0.0333h)_3/0.35h)_2/(0.0333h)_3]$	$[(p_3/q)_2/p_3]$		$p^0(\alpha) = p_u^0 \sin(\pi\alpha/L_\alpha)$ if $0 \le \alpha \le L_\alpha$	5	–
b$^{(*§)}$	$[90/0]$	$[0.5h/0.5h]$	$[r_2]$		$p^0(\alpha) = p_u^0 \sin(\pi\alpha/L_\alpha)$ if $0 \le \alpha \le L_\alpha$	4	-
c$^{(*§)}$	$[0]_{11}$	$[0.01h/0.025h/0.015h/0.02h/0.03h/0.4h]_S$	$[s1/s2/s3/s1/s3/s4]_S$		$p^0(\alpha) = p_u^0 \sin(\pi\alpha/L_\alpha)$ if $0 \le \alpha \le L_\alpha$	4	-
d$^{(*§)}$	$[0/-90/0/-90]$	$[0.25h]_4$	$[p]_4$		$p^0(\alpha) = p_u^0 \sin(\pi\alpha/L_\alpha)$ if $0 \le \alpha \le L_\alpha$	4	-
e$^{(*\square§)}$	$[0/0/0]$	$[0.1h/0.7h/0.2h]$	$[c1/c1/c1]$		$p^0(\alpha,\beta) = p_u^0 \sin(\pi\alpha/L_\alpha)\sin(\pi\beta/L_\beta)$ if $0 \le \alpha \le L_\alpha$ and $0 \le \beta \le L_\beta$	4	3
f$^{(*§)}$	$[0/0/0]$	$[(2h/7)/(4h/7)/(h/7)]$	$[n/n/n]$		$p^0(\alpha) = p_u^0$ if $0 \le \alpha \le L_\alpha$	5.714	–
g$^{(*§)}$	$[0/0/0]$	$[(2h/7)/(4h/7)/(h/7)]$	$[n/n/n]$			20	–
h$^{(*§)}$	$[0/0/0]$	$[(2h/7)/(4h/7)/(h/7)]$	$[n/n/n]$	support at $\alpha = 0.9L\alpha$	$p^0(\alpha) = p_u^0$ if $0 \le \alpha \le L_\alpha$	5.714	–
i$^{(§)}$	$[0/0/0]$	$[0.2h/0.7h/0.1h]$	$[c2/c2/c2]$		$p^0(\alpha,\beta) = p_u^0 \sin(\pi\alpha/L_\alpha)\sin(\pi\beta/L_\beta)$ if $0 \le \alpha \le L_\alpha$ and $0 \le \beta \le L_\beta$	4	3
j$^{(*\square§)}$	$[0/0/0/0]$	$[0.05h/0.15h/0.70h/0.10h]$	$[p/mc/mc/p]$			4	1
k$^{(*§)}$	$[0/0/0]$	$[0.05h/0.9h/0.05h]$	$[i1/i2/i1]$		$p^0(\alpha,\beta) = p_u^0$ if $\begin{cases} L_\alpha/4 \le \alpha \le 3L_\alpha/4 \\ L_\beta/4 \le \beta \le 3L_\beta/4 \end{cases}$	5	1

Whether Murakami's function assumption is not satisfied by u_α (*), u_β ($\square$) and u_ς (§)

$$\partial \Pi_{HW}^g = \int_V \left[(\varepsilon_{ij}^u - \varepsilon_{ij})\partial\sigma_{ij} + (\sigma_{ij}^e - \sigma_{ij})\partial\varepsilon_{ij} + \sigma_{ij}\partial\varepsilon_{ij}^u - b_i\partial u_i \right]dv - \int_{S_t} \tilde{t}_i \partial u_i ds - \int_{S_u} \left[(u_i - \tilde{u}_i)n_j\partial\sigma_{ij} + \sigma_{ij}n_j\partial u_i \right]ds = 0 \tag{1}$$

The components of the external unit normal to the volume bounding surface are represented by n_j, b_i are the components of body forces and terms $\int_V (\varepsilon_{ij}^u - \varepsilon_{ij})\partial\sigma_{ij}dv$, $\int_V (\sigma_{ij}^e - \sigma_{ij})\partial\varepsilon_{ij}dv$ constitute the compatibility relations that ensure the consistency of assumed strain and stress fields with their counterparts obtained from stress-strain and strain-displacement relations.

Theories assuming displacement and stress fields as primary variables are developed using Hellinger-Reissner *HR* canonical functional:

$$\partial \Pi_{HR} = \int_V \left[\sigma_{ij}\partial\varepsilon_{ij}^u + (\gamma_{i3}^u - \gamma_{i3}^\sigma)\partial\sigma_{i3} + (\varepsilon_{33}^u - \hat{\varepsilon}_{33}^\sigma)\partial\sigma_{33} - b_i\partial u_i \right]dv - \int_{S_t} \tilde{t}_i\partial u_i ds - \int_{S_u} \left[(u_i - \tilde{u}_i)n_j\partial\sigma_{ij} + \sigma_{ij}n_j\partial u_i \right]ds = 0 \tag{2}$$

The following definitions apply: $i, j = 1, 2 \equiv x, y$; $3 \equiv z$; $\gamma_{ij(i3)(33)} = 2\varepsilon_{ij(i3)(33)}$; $\hat{\varepsilon}_{33}^\sigma = 1/C_{3333}(\sigma_{33} - C_{33ij}\varepsilon_{ij}^u)$.

Theories in displacement-based form are derived using the Total Potential Energy functional.

The middle-plane displacement components u^0, v^0, w^0 in the α, β, ς directions and the rotations of the normal $\theta_\alpha = \Gamma_\alpha^0(\alpha, \beta) - w^0(\alpha, \beta)_{,\alpha}$, $\theta_\beta = \Gamma_\beta^0(\alpha, \beta) - w^0(\alpha, \beta)_{,\beta}$ are assumed as the only functional degrees of freedom.

2.3. Trial functions

Closed form solutions are obtained within the framework of Rayleigh-Ritz method, in conjunction with Lagrange multipliers method. Accordingly, d.o.f. are expressed as a truncated series expansion of unknown amplitudes A_Δ^i and trial functions $\Re^i(\alpha, \beta)$ that individually satisfy the prescribed boundary conditions:

$$\Delta = \sum_{i=1}^{m_\Delta} A_\Delta^i \Re^i(\alpha, \beta) \tag{3}$$

Table 3

Normalization of displacements and stresses, expansion order and trial functions.

Case Meshing $[\alpha_a \cdot \beta_b \cdot \varsigma_h]^{(+)}$	Normalization	Expansion	Trial function
a $[16 \cdot 2 \cdot 60]$	$\overline{u_\alpha} = \frac{E_2 u_\alpha(0,\varsigma)}{hp^0}$ $\overline{u_\varsigma} = \frac{100 E_2 h^3 u_\varsigma(\frac{L_\alpha}{2},\varsigma)}{L_\alpha^4 p^0}$ $\overline{\sigma_{\alpha\alpha}} = \frac{\sigma_{\alpha\alpha}(\frac{L_\alpha}{2},\varsigma)}{p^0}$ $\overline{\sigma_{\alpha\varsigma}} = \frac{\sigma_{\alpha\varsigma}(0,\varsigma)}{p^0}$	1	$u^0(\alpha) = \sum_{m=1}^{M} A_m \cos(\frac{m\pi\alpha}{L_\alpha})$;
b $[16 \cdot 2 \cdot 60]$	$\overline{u_\alpha} = \frac{E_2 u_\alpha(0,\varsigma)}{hp^0}$ $\overline{u_\varsigma} = \frac{100 E_2 h^3 u_\varsigma(\frac{L_\alpha}{2},\varsigma)}{L_\alpha^4 p^0}$ $\overline{\sigma_{\alpha\alpha}} = \frac{\sigma_{\alpha\alpha}(\frac{L_\alpha}{2},\varsigma)}{p^0}$ $\overline{\sigma_{\alpha\varsigma}} = \frac{\sigma_{\alpha\varsigma}(0,\varsigma)}{p^0}$ $\overline{\sigma_{\varsigma\varsigma}} = \frac{\sigma_{\varsigma\varsigma}(\frac{L_\alpha}{2},\varsigma)}{p^0}$	1	$w^0(\alpha) = \sum_{m=1}^{M} C_m \sin(\frac{m\pi\alpha}{L_\alpha})$;
c $[16 \cdot 2 \cdot 60]$	$\overline{u_\alpha} = \frac{u_\alpha(L_\alpha,\varsigma)}{hp^0}$ $\overline{u_\varsigma} = \frac{u_\varsigma(L_\alpha,\varsigma)}{hp^0}$ $\overline{\sigma_{\alpha\alpha}} = \frac{\sigma_{\alpha\alpha}(L_\alpha,\varsigma)}{p^0(L_\alpha/h)^2}$ $\overline{\sigma_{\alpha\varsigma}} = \frac{\sigma_{\alpha\varsigma}(L_\alpha,\varsigma)}{p^0}$ $\overline{\sigma_{\varsigma\varsigma}} = \frac{\sigma_{\varsigma\varsigma}(L_\alpha,\varsigma)}{p^0}$	1	$\Gamma_\alpha^0(\alpha) = \sum_{m=1}^{M} D_m \cos(\frac{m\pi\alpha}{L_\alpha})$
d $[16 \cdot 2 \cdot 60]$	$\overline{u_\alpha} = \frac{E_2 u_\alpha(0,\varsigma)}{hp^0}$ $\overline{u_\varsigma} = \frac{u_\varsigma(\frac{L_\alpha}{2},\varsigma)}{hp^0}$ $\overline{\sigma_{\alpha\alpha}} = \frac{\sigma_{\alpha\alpha}(\frac{L_\alpha}{2},\varsigma)}{p^0}$ $\overline{\sigma_{\alpha\varsigma}} = \frac{\sigma_{\alpha\varsigma}(0,\varsigma)}{p^0}$ $\overline{\sigma_{\varsigma\varsigma}} = \frac{\sigma_{\varsigma\varsigma}(\frac{L_\alpha}{2},\varsigma)}{p^0}$	1	
e $[10 \cdot 10 \cdot 28]$	$\overline{u_\alpha} = \frac{u_\alpha(0,\frac{L_\beta}{2},\varsigma)E_{1MATbc}h^2}{p^0 L_\alpha^3}$ $\overline{u_\beta} = \frac{u_\beta(\frac{L_\alpha}{2},0,\varsigma)}{hp^0}$ $\overline{u_\varsigma} = \frac{u_\varsigma(\frac{L_\alpha}{2},\frac{L_\beta}{2},\varsigma)}{hp^0}$ $\overline{\sigma_{\alpha\alpha}} = \frac{\sigma_{\alpha\alpha}(\frac{L_\alpha}{2},\frac{L_\beta}{2},\varsigma)}{p^0(L_\alpha/h)^2}$ $\overline{\sigma_{\beta\beta}} = \frac{\sigma_{\beta\beta}(\frac{L_\alpha}{2},\frac{L_\beta}{2},\varsigma)}{p^0(L_\alpha/h)^2}$ $\overline{\sigma_{\alpha\beta}} = \frac{\sigma_{\alpha\beta}(0,0,\varsigma)}{p^0(L_\alpha/h)^2}$ $\overline{\sigma_{\alpha\varsigma}} = \frac{\sigma_{\alpha\varsigma}(0,\frac{L_\beta}{2},\varsigma)h}{p^0 L_\alpha}$ $\overline{\sigma_{\beta\varsigma}} = \frac{\sigma_{\beta\varsigma}(\frac{L_\alpha}{2},0,\varsigma)}{p^0}$ $\overline{\sigma_{\varsigma\varsigma}} = \frac{\sigma_{\varsigma\varsigma}(\frac{L_\alpha}{2},\frac{L_\beta}{2},\varsigma)}{p^0}$	1	$u^0(\alpha,\beta) = \sum_{m=1}^{M}\sum_{n=1}^{N} A_{mn} \cos(\frac{m\pi}{L_\alpha}\alpha)\sin(\frac{n\pi}{L_\beta}\beta)$; $v^0(\alpha,\beta) = \sum_{m=1}^{M}\sum_{n=1}^{N} B_{mn} \sin(\frac{m\pi}{L_\alpha}\alpha)\cos(\frac{n\pi}{L_\beta}\beta)$; $w^0(\alpha,\beta) = \sum_{m=1}^{M}\sum_{n=1}^{N} C_{mn} \sin(\frac{m\pi}{L_\alpha}\alpha)\sin(\frac{n\pi}{L_\beta}\beta)$; $\Gamma_\alpha^0(\alpha,\beta) = \sum_{m=1}^{M}\sum_{n=1}^{N} D_{mn} \cos(\frac{m\pi}{L_\alpha}\alpha)\sin(\frac{n\pi}{L_\beta}\beta)$; $\Gamma_\beta^0(\alpha,\beta) = \sum_{m=1}^{M}\sum_{n=1}^{N} E_{mn} \sin(\frac{m\pi}{L_\alpha}\alpha)\cos(\frac{n\pi}{L_\beta}\beta)$;
i $[10 \cdot 10 \cdot 28]$	$\overline{u_\alpha} = \frac{u_\alpha(0,\frac{L_\beta}{2},\varsigma)}{hp^0}$ $\overline{u_\beta} = \frac{u_\beta(\frac{L_\alpha}{2},0,\varsigma)}{hp^0}$ $\overline{u_\varsigma} = \frac{u_\varsigma(\frac{L_\alpha}{2},\frac{L_\beta}{2},\varsigma)}{hp^0}$ $\overline{\sigma_{\alpha\alpha}} = \frac{\sigma_{\alpha\alpha}(\frac{L_\alpha}{2},\frac{L_\beta}{2},\varsigma)}{p^0(L_\alpha/h)^2}$ $\overline{\sigma_{\beta\beta}} = \frac{\sigma_{\beta\beta}(\frac{L_\alpha}{2},\frac{L_\beta}{2},\varsigma)}{p^0(L_\alpha/h)^2}$	1	
j $[10 \cdot 10 \cdot 28]$	$\overline{\sigma_{\alpha\beta}} = \frac{\sigma_{\alpha\beta}(0,0,\varsigma)}{p^0(L_\alpha/h)^2}$ $\overline{\sigma_{\alpha\varsigma}} = \frac{\sigma_{\alpha\varsigma}(0,\frac{L_\beta}{2},\varsigma)}{p^0}$ $\overline{\sigma_{\beta\varsigma}} = \frac{\sigma_{\beta\varsigma}(\frac{L_\alpha}{2},0,\varsigma)}{p^0}$ $\overline{\sigma_{\varsigma\varsigma}} = \frac{\sigma_{\varsigma\varsigma}(\frac{L_\alpha}{2},\frac{L_\beta}{2},\varsigma)}{p^0}$	1	
k $[10 \cdot 10 \cdot 28]$	$\overline{u_\alpha} = \frac{u_\alpha(0,\frac{L_\beta}{2},\varsigma)}{hp^0}$ $\overline{u_\beta} = \frac{u_\beta(\frac{L_\alpha}{2},0,\varsigma)}{hp^0}$ $\overline{u_\varsigma} = \frac{u_\varsigma(\frac{L_\alpha}{2},\frac{L_\beta}{2},\varsigma)}{hp^0}$ $\overline{\sigma_{\alpha\alpha}} = \frac{\sigma_{\alpha\alpha}(\frac{L_\alpha}{2},\frac{L_\beta}{2},\varsigma)}{p^0(L_\alpha/h)^2}$ $\overline{\sigma_{\beta\beta}} = \frac{\sigma_{\beta\beta}(\frac{L_\alpha}{2},\frac{L_\beta}{2},\varsigma)}{p^0(L_\alpha/h)^2}$ $\overline{\sigma_{\alpha\beta}} = \frac{\sigma_{\alpha\beta}(0,0,\varsigma)}{p^0(L_\alpha/h)^2}$ $\overline{\sigma_{\alpha\varsigma}} = \frac{\sigma_{\alpha\varsigma}(0,\frac{L_\beta}{2},\varsigma)}{p^0}$ $\overline{\sigma_{\beta\varsigma}} = \frac{\sigma_{\beta\varsigma}(\frac{L_\alpha}{2},0,\varsigma)}{p^0}$ $\overline{\sigma_{\varsigma\varsigma}} = \frac{\sigma_{\varsigma\varsigma}(\frac{L_\alpha}{2},\frac{L_\beta}{2},\varsigma)}{p^0}$	20	
f $[20 \cdot 2 \cdot 60]$	$\overline{u_\alpha} = \frac{u_\alpha(L_\alpha,\varsigma)}{hp^0}$ $\overline{u_\varsigma} = \frac{u_\varsigma(L_\alpha,\varsigma)}{hp^0}$ $\overline{\sigma_{\alpha\alpha}} = \frac{\sigma_{\alpha\alpha}(L_\alpha,\varsigma)}{p^0(L_\alpha/h)^2}$ $\overline{\sigma_{\alpha\varsigma}} = \frac{A\sigma_{\alpha\varsigma}(L_\alpha,\varsigma)}{P^0 L_\alpha}$ $\overline{\sigma_{\varsigma\varsigma}} = \frac{\sigma_{\varsigma\varsigma}(L_\alpha,\varsigma)}{p^0}$	9	$u^0(\alpha) = \sum_{i=1}^{l} A_i (\frac{\alpha}{L_\alpha})^i$;
g $[20 \cdot 2 \cdot 60]$	$\overline{u_\alpha} = \frac{u_\alpha(L_\alpha,\varsigma)}{hp^0}$ $\overline{u_\varsigma} = \frac{u_\varsigma(L_\alpha,\varsigma)}{hp^0}$ $\overline{\sigma_{\alpha\alpha}} = \frac{\sigma_{\alpha\alpha}(L_\alpha,\varsigma)}{p^0(L_\alpha/h)^2}$ $\overline{\sigma_{\alpha\varsigma}} = \frac{A\sigma_{\alpha\varsigma}(L_\alpha,\varsigma)}{P^0 L_\alpha}$ $\overline{\sigma_{\varsigma\varsigma}} = \frac{\sigma_{\varsigma\varsigma}(L_\alpha,\varsigma)}{p^0}$	9	$w^0(\alpha) = \sum_{i=1}^{l} C_i (\frac{\alpha}{L_\alpha})^i$;
h $[20 \cdot 2 \cdot 60]$	$\overline{u_\alpha} = \frac{u_\alpha(0.89L_\alpha,\varsigma)}{hp^0}$ $\overline{u_\varsigma} = \frac{u_\varsigma(0.89L_\alpha,\varsigma)}{hp^0}$ $\overline{\sigma_{\alpha\alpha}} = \frac{\sigma_{\alpha\alpha}(0.89L_\alpha,\varsigma)}{p^0(L_\alpha/h)^2}$ $\overline{\sigma_{\alpha\varsigma}} = \frac{\sigma_{\alpha\varsigma}(0.89L_\alpha,\varsigma)}{p^0}$ $\overline{\sigma_{\varsigma\varsigma}} = \frac{\sigma_{\varsigma\varsigma}(0.89L_\alpha,\varsigma)}{p^0}$	9	$\Gamma_\alpha^0(\alpha) = \sum_{i=1}^{l} D_i (\frac{\alpha}{L_\alpha})^i$

Cases with the same trial functions are listed together. $^{(+)}$A uniform mesh is used; α_a and β_b represent the number of elements in α and β directions, respectively, ς_h is the number of elements across the thickness;

where Δ symbolizes in turns u^0, v^0, w^0, Γ_α^0, Γ_β^0. The trial functions are explicitly defined in Table 3 for each specific case along with the expansion order and normalizations used. As a consequence, an algebraic system is obtained, whose solution provides the numerical value of each amplitude, from which displacement, strain and stress fields can be constructed.

The same boundary conditions and the same representation are shared by all theories, in order to compare them under the same conditions. In details, at the clamped edge of cantilever beams, hereafter assumed at $\alpha = 0$ by way of example, the following conditions are enforced

$$u^0(0,0) = 0; \qquad w^0(0,0) = 0; \qquad w^0(0,0)_{,\alpha} = 0; \qquad \Gamma_\alpha^0(0,0) = 0 \tag{4}$$

In order to simulate that (4) holds identically across the thickness, the following further conditions are enforced:

$$u_\alpha(0,\varsigma)_{,\varsigma} = 0; \qquad u_\varsigma(0,\varsigma)_{,\varsigma} = 0; \qquad u_\varsigma(0,\varsigma)_{,\alpha\varsigma} = 0 \tag{5}$$

Using Lagrange multipliers method, it is further enforced

$$\int_{-h/2}^{h/2} \sigma_{\alpha\varsigma}(0,\varsigma)d\varsigma = T \tag{6}$$

to ensure that the transverse shear stress resultant force equals the constraint force, while at the free edge $\alpha = L$ (L is the beam length) this resultant force is enforced to vanish

$$\int_{-h/2}^{h/2} \sigma_{\alpha\varsigma}(L,\varsigma)d\varsigma = 0 \tag{7}$$

No conditions are enforced on bending moments, but if necessary they could be coerced choosing a sufficient expansion order in (3).

At the clamped edge of propped-cantilever beams, the previous boundary conditions still hold, while at $\alpha = L$ the following support condition is enforced at the lower face $\varsigma = -h/2$

$$w^0(L, -h/2) = 0 \tag{8}$$

while condition (7) is reformulated as:

$$\int_{-h/2}^{h/2} \sigma_{\alpha\varsigma}(L, \varsigma)d\varsigma = T_L \tag{9}$$

Instead, at simply-supported edges, the following boundary conditions are enforced

$$w^0(0, \beta) = 0; \qquad w^0(L_\alpha, \beta) = 0; \qquad w^0(0, \beta)_{,\alpha\alpha} = 0; \qquad w^0(L_\alpha, \beta)_{,\alpha\alpha} = 0$$

$$w^0(\alpha, 0) = 0; \qquad w^0(\alpha, L_\beta) = 0; \qquad w^0(\alpha, 0)_{,\beta\beta} = 0; \qquad w^0(\alpha, L_\beta)_{,\beta\beta} = 0 \tag{10}$$

on the reference mid-plane of the plate. With appropriate simplifications, corresponding ones for simply-supported beams are obtained.

As specified below, symbolic calculus is used for generating governing equations. An advantage offered by this technique is that loading does not require to be expressed as a series expansion like variables (3), just its mathematical formula being used, so a computational advantage is achieved irrespective it is continuous, discontinuous, or locally applied.

2.4. The ZZA displacement-based theory

Hereafter the theoretical framework of ZZA [26] is briefly expounded, being the basis for theories developed and assessed in this paper. The through-thickness displacement field is postulated as:

$$u_\alpha(\alpha, \beta, \varsigma) = \left[u_\alpha^0(\alpha, \beta) + \varsigma\left(\Gamma_\alpha^0(\alpha, \beta) - w^0(\alpha, \beta)_{,\alpha} \right) \right]_0 + \left[F_\alpha^u(\alpha, \beta, \varsigma) \right]_i$$

$$+ \left[\sum_{k=1}^{n_i} \Phi_\alpha^k(\alpha, \beta)(\varsigma - \varsigma_k)H_k(\varsigma) + \sum_{j=1}^{n_\Im} {}_\alpha C_u^j(\alpha, \beta)H_j(\varsigma) \right]_c$$

$$u_\varsigma(\alpha, \beta, \varsigma) = \left[w^0(\alpha, \beta) \right]_0 + \left[F^\varsigma(\alpha, \beta, \varsigma) \right]_i + \left[\sum_{k=1}^{n_i} \Psi^k(\alpha, \beta)(\varsigma - \varsigma_k)H_k(\varsigma) \right.$$

$$\left. + \sum_{k=1}^{n_i} \Omega^k(\alpha, \beta)(\varsigma - \varsigma_k)^2 H_k(\varsigma) + \sum_{j=1}^{n_\Im} C_\varsigma^j(\alpha, \beta)H_j(\varsigma) \right]_c \tag{11}$$

Three kinds of contributions are incorporated, namely lower-, and higher-order ones, i.e. $[...]_0$, $[...]_i$ respectively, and layerwise functions $[...]_c$. Contribution $[...]_0$, which is linear in u_α and uniform across the thickness in u_ς, contains the only five functional degrees of freedom.

Functions $[F_\alpha^u]_i$, $[F^\varsigma]_i$ aren't just depending on ς because apexes and subscript $_\alpha^u$, $^\varsigma$ represent the functional dependence on the d.o.f. that themselves are function of in-plane coordinates. Such functions are expressed as a series expansion of functions of ς (assumed as desired) and unknown coefficients, as described immediately after.

Any combination of independent functions could be assumed, however to include theory [19] as a particular case of ZZA, the following power series expansion is chosen:

$$\left[F_\alpha^u(\alpha, \beta, \varsigma) \right]_i = \left[C_\alpha^i(\alpha, \beta)\varsigma^2 + D_\alpha^i(\alpha, \beta)\varsigma^3 + (O\varsigma^4...) \right]_i = \left[{}_3(\tilde{.})_\alpha \right]_i + \left[(O\varsigma^4...) \right]_i$$

$$\left[F^\varsigma(\alpha, \beta, \varsigma) \right]_i = \left[b^i(\alpha, \beta)\varsigma + c^i(\alpha, \beta)\varsigma^2 + d^i(\alpha, \beta)\varsigma^3 + e^i(\alpha, \beta)\varsigma^4 + (O\varsigma^5...) \right]_i = \left[{}_4(\tilde{.})_\varsigma \right]_i + \left[(O\varsigma^5...) \right]_i \tag{12}$$

Higher-order contributions $\left[(O\varsigma^4...) \right]_i$, $\left[(O\varsigma^5...) \right]_i$ are characteristic of ZZA, while $\left[{}_3(\tilde{.})_\alpha \right]_i$, $\left[{}_4(\tilde{.})_\varsigma \right]_i$ are the same as in the previous model [19].

The contributions by (12) are indicated as U_α^i, U_ς^i and are rearranged in the following way:

$$U_\alpha^i(\alpha, \beta, \varsigma) = \left[A_{\alpha2}\varsigma^2 + A_{\alpha3}\varsigma^3 \right] + A_{\alpha4}\varsigma^4 + \cdots + A_{\alpha n}\varsigma^n$$

$$U_\zeta^i(\alpha, \beta, \varsigma) = \left[A_{\varsigma1}\varsigma + A_{\varsigma2}\varsigma^2 + A_{\varsigma3}\varsigma^3 + A_{\varsigma4}\varsigma^4 \right] + A_{\varsigma5}\varsigma^5 + \cdots + A_{\varsigma n}\varsigma^n \tag{13}$$

in order to obtain exact expressions of coefficients via symbolic calculus. Ones under square brackets are determined by enforcing the fulfillment of boundary conditions

$$\sigma_{\alpha\varsigma} = \sigma_{\varsigma\varsigma,\varsigma} = 0; \qquad \sigma_{\varsigma\varsigma} = p_{(\pm)}^0 \tag{14}$$

Here $p_{(\pm)}^0$ represents the distributed transverse loading acting on upper $p_{(+)}^0$ and lower $p_{(-)}^0$ faces.

Of course, also non-homogeneous conditions $\sigma_{\alpha\varsigma}$; $\sigma_{\beta\varsigma} \neq 0$ could be enforced without any additional difficulty. The expressions of remaining contributions of (13) outside square brackets are obtained by enforcing the fulfillment of local equilibrium equations

$$\sigma_{\alpha\beta,\beta} + \sigma_{\alpha\varsigma,\varsigma} = b_\alpha; \qquad \sigma_{\alpha\varsigma,\alpha} + \sigma_{\varsigma\varsigma,\varsigma} = b_\varsigma \tag{15}$$

at selected points across the thickness (where appropriate, only a partial set). The in-plane position where (15) are computed can be chosen suitably for each case.

Higher-order contributions (13) enable a variable-kinematics representation keeping the overall number of d.o.f. fixed to five, irrespective of the number of constituent or computational layers. A single computational layer proved to be effective in the numerical applications, as it already supplies a suitable number of equilibrium points.

The expressions of zig-zag amplitudes Φ_α^k, Ψ^k and Ω^k included into contributions $[\ldots]_c$ are determined by enforcing the stress compatibility conditions

$$\sigma_{\alpha\varsigma}\big(^{(k)}\varsigma^+\big) = \sigma_{\alpha\varsigma}\big(^{(k)}\varsigma^-\big); \qquad \sigma_{\varsigma\varsigma}\big(^{(k)}\varsigma^+\big) = \sigma_{\varsigma\varsigma}\big(^{(k)}\varsigma^-\big); \qquad \sigma_{\varsigma\varsigma,\varsigma}\big(^{(k)}\varsigma^+\big) = \sigma_{\varsigma\varsigma,\varsigma}\big(^{(k)}\varsigma^-\big) \tag{16}$$

at physical and mathematical layer interfaces, which directly follow from (15). Φ_α^k enable the continuity of transverse shears, while Ψ^k, Ω^k enable the continuity of the transverse normal stress and of its gradient. All together provide the right slope changes of displacements at the interfaces of layers with different material properties and/or orientation. Note that $(\varsigma - \varsigma_k)H_k$ in (11) is Di Sciuva's zig-zag function [14] while $(\varsigma - \varsigma_k)^2 H_k$ is Icardi's parabolic zig-zag function [19], H_k being the Heaviside unit step function ($H_k = 0$ for $\varsigma < \varsigma_k$, while $H_k = 1$ for $\varsigma \geq \varsigma_k$). The enforcement of the stress compatibility conditions (16) yields to a system of algebraic equations at each interface that is solved using symbolic calculus. In this way, closed form expressions of zig-zag amplitudes are obtained once and for all in terms of elastic properties of layers and of d.o.f. derivatives. The technique of construction of structural model via symbolic calculus is described in Appendix A. If just material properties and/or the orientation of layers change, not their number, symbolic expressions remain the same and therefore need not be recalculated.

Layerwise contributions $_\alpha C_u^j$ and C_ς^j restore the continuity of displacements at physical or mathematical layer interfaces:

$$u_\alpha\big(^{(k)}\varsigma^+\big) = u_\alpha\big(^{(k)}\varsigma^-\big); \qquad u_\varsigma\big(^{(k)}\varsigma^+\big) = u_\varsigma\big(^{(k)}\varsigma^-\big) \tag{17}$$

Since the expressions of the initially unknown coefficients appearing in (11) are all redefined across the thickness, as outlined above, ZZA and the theories with this same characteristic considered hereafter are named "adaptive" theories, as they can adapt to the variation of solutions across the thickness.

In conclusion, it should be noted that SEUPT technique [49] may be used to obtain a C° formulation of the ZZA and of the following theories suitable for development of finite elements.

2.4.1. New theories derived from ZZA

New displacement-based theories that derive from ZZA are developed hereafter with the purpose to investigate the effects of the choice of representation and zig-zag functions on accuracy. The first theory, here referred as ZZA1, postulates the following displacement field:

$$u_\alpha(\alpha, \beta, \varsigma) = \big[u_\alpha^0(\alpha, \beta) + \varsigma\big(\Gamma_\alpha^0(\alpha, \beta) - w^0(\alpha, \beta),_\alpha\big)\big]_0 + \big[C_\alpha^i(\alpha, \beta)\varsigma^2 + D_\alpha^i(\alpha, \beta)\varsigma^3 + \Phi_\alpha^i(\alpha, \beta)\varsigma +_\alpha C_u^i(\alpha, \beta)\big]_{i+c}$$

$$u_\varsigma(\alpha, \beta, \varsigma) = \big[w^0(\alpha, \beta)\big]_0 + \big[b^i(\alpha, \beta)\varsigma + c^i(\alpha, \beta)\varsigma^2 + d^i(\alpha, \beta)\varsigma^3 + e^i(\alpha, \beta)\varsigma^4\big]_i$$

$$+ \left[\sum_{k=1}^{n_i} \Psi^k(\alpha, \beta)(\varsigma - \varsigma_k)H_k(\varsigma) + \sum_{k=1}^{n_i} \Omega^k(\alpha, \beta)(\varsigma - \varsigma_k)^2 H_k(\varsigma) + \sum_{j=1}^{n_\Im} C_\varsigma^j(\alpha, \beta)H_j(\varsigma)\right]_c \tag{18}$$

The transverse displacement is the same of ZZA, while zig-zag functions of in-plane displacements are omitted because coefficients $\Phi_\alpha^i(\alpha, \beta)$ and $_\alpha C_u^i(\alpha, \beta)$, can be determined through the enforcement of (16) to (17). On the other hand, $C_\alpha^i(\alpha, \beta)$ and $D_\alpha^i(\alpha, \beta)$ are calculated by imposing (14) and (15), so, the full set of physical constraints is enforced.

The purpose of this study is to demonstrate that results that are indistinguishable from those of ZZA can be obtained, thus proving that the choice of zig-zag functions is immaterial whenever the whole set of constraints (14) to (17) is enforced and exact relations are computed via symbolic calculus.

To corroborate the previous conclusions, another new theory, called ZZA2, is developed from ZZA as:

$$u_\alpha(\alpha, \beta, \varsigma) = \big[u_\alpha^0(\alpha, \beta) + \varsigma\big(\Gamma_\alpha^0(\alpha, \beta) - w^0(\alpha, \beta),_\alpha\big)\big]_0 + \big[C_\alpha^i(\alpha, \beta)\varsigma^2 + D_\alpha^i(\alpha, \beta)\varsigma^3\big]_i$$

$$+ \left[\sum_{k=1}^{n_i} \Phi_\alpha^k(\alpha, \beta)(\varsigma - \varsigma_k)H_k(\varsigma) + \sum_{j=1}^{n_\Im} {}_\alpha C_u^j(\alpha, \beta)H_j(\varsigma)\right]_c$$

$$u_\varsigma(\alpha, \beta, \varsigma) = \big[w^0(\alpha, \beta)\big]_0 + \big[b^i(\alpha, \beta)\varsigma + c^i(\alpha, \beta)\varsigma^2 + d^i(\alpha, \beta)\varsigma^3 + e^i(\alpha, \beta)\varsigma^4 + C_\varsigma^i(\alpha, \beta)\big]_{i+c} \tag{19}$$

In-plane displacements are the same as ZZA, while zig-zag contributions are omitted within the transverse displacement because their role is played by redefining coefficients $b^i(\alpha, \beta)$ and $c^i(\alpha, \beta)$ across the thickness through the enforcement of (16) (for layers with $i > 1$). $C_\varsigma^j(\alpha, \beta)$ are calculated by imposing (17), while the remaining coefficients are determined by enforcing (14) and (15). So (19) can be viewed as the dual form of (18), due to the exchange of displacements that do not contain zig-zag contributions.

Numerical applications will prove that also (19) gives results coincident with those of ZZA, although having different piecewise contributions, so again it will be demonstrated that the choice of zig-zag functions is immaterial whenever the whole set of constraints (14) to (17) is enforced.

A further theory called ZZA3 is developed as:

$$u_\alpha(\alpha, \beta, \varsigma) = \big[u_\alpha^0(\alpha, \beta) + \varsigma\big(\Gamma_\alpha^0(\alpha, \beta) - w^0(\alpha, \beta),_\alpha\big)\big]_0 + \big[C_\alpha^i(\alpha, \beta)\cos(\varsigma/h) + D_\alpha^i(\alpha, \beta)\sin(\varsigma/h)\big]_i$$

$$+ \left[\sum_{k=1}^{n_i} \Phi_\alpha^k(\alpha, \beta)(\varsigma - \varsigma_k)H_k(\varsigma) + \sum_{j=1}^{n_\Im} {}_\alpha C_u^j(\alpha, \beta)H_j(\varsigma)\right]_c$$

$$u_\varsigma(\alpha,\beta,\varsigma) = \left[w^0(\alpha,\beta)\right]_0 + \left[b^i(\alpha,\beta)(\varsigma/h) + c^i(\alpha,\beta)e^{(\varsigma/h)} + d^i(\alpha,\beta)\cos(\varsigma/h) + e^i(\alpha,\beta)\sin(\varsigma/h)\right]_i$$
$$+ \left[\sum_{k=1}^{n_i} \Psi^k(\alpha,\beta)(\varsigma-\varsigma_k)H_k(\varsigma) + \sum_{k=1}^{n_i} \Omega^k(\alpha,\beta)(\varsigma-\varsigma_k)^2 H_k(\varsigma) + \sum_{j=1}^{n_\Im} C_\varsigma^j(\alpha,\beta)H_j(\varsigma)\right]_c \quad (20)$$

which derives from (11) through a different choice of the representation functions across the thickness. Such functions are chosen as a mixture of trigonometric and exponential functions randomly selected, since studies [18] and [31–39] have highlighted this choice can considerably affect accuracy. On the contrary, results by [29] and [48] indicate that this choice is immaterial if exact expressions of coefficients are obtained via symbolic calculus and the full set of constraints (14) to (17) is enforced. This will also be confirmed by the numerical results of (20), therefore that the choice of the representation functions is also immaterial. On the contrary, the results of theories that only partially satisfy (14) to (17) show a strong sensitivity of results accuracy, as in [18] and [31–39].

In order to corroborate this, two more theories are considered in the numerical illustrations. The first one, which is retaken from [19] and is called ZZ_NA1, has the following displacement field:

$$u_\alpha(\alpha,\beta,\varsigma) = \left[u_\alpha^0(\alpha,\beta) + \varsigma\left(\Gamma_\alpha^0(\alpha,\beta) - w^0(\alpha,\beta)_{,\alpha}\right)\right]_0 + \left[C_\alpha(\alpha,\beta)\varsigma^2 + D_\alpha(\alpha,\beta)\varsigma^3\right]_i + \left[\sum_{k=1}^{n_i} \Phi_\alpha^k(\alpha,\beta)(\varsigma-\varsigma_k)H_k(\varsigma)\right]_c$$

$$u_\varsigma(\alpha,\beta,\varsigma) = \left[w^0(\alpha,\beta)\right]_0 + \left[b(\alpha,\beta)\varsigma + c(\alpha,\beta)\varsigma^2 + d(\alpha,\beta)\varsigma^3 + e(\alpha,\beta)\varsigma^4\right]_i$$
$$+ \left[\sum_{k=1}^{n_i} \Psi^k(\alpha,\beta)(\varsigma-\varsigma_k)H_k(\varsigma) + \sum_{k=1}^{n_i} \Omega^k(\alpha,\beta)(\varsigma-\varsigma_k)^2 H_k(\varsigma)\right]_c \quad (21)$$

Differently to previous theories, higher-order coefficients within $[...]_i$ are not recomputed across the thickness, but zig-zag amplitudes are still recomputed by imposing (16). So, differently to ZZA and ZZA1 to ZZA3 not all terms are redefined across the thickness. For this reason, (21) is only capable of partially satisfying (14) to (17), consequently its results are inaccurate unless many computational layers are used.

Another theory, called ZZ_NA2 is proposed that considers a further different kind of representation across the thickness as:

$$u_\alpha(\alpha,\beta,\varsigma) = \left[u_\alpha^0(\alpha,\beta) + \varsigma\left(\Gamma_\alpha^0(\alpha,\beta) - w^0(\alpha,\beta)_{,\alpha}\right)\right]_0 + \left[C_\alpha(\alpha,\beta)\cos(\varsigma/h) + D_\alpha(\alpha,\beta)\sin(\varsigma/h)\right]_i$$
$$+ \left[\sum_{k=1}^{n_i} \Phi_\alpha^k(\alpha,\beta)(\varsigma-\varsigma_k)H_k(\varsigma)\right]_c$$

$$u_\varsigma(\alpha,\beta,\varsigma) = \left[w^0(\alpha,\beta)\right]_0 + \left[b(\alpha,\beta)(\varsigma/h) + c(\alpha,\beta)e^{(\varsigma/h)} + d(\alpha,\beta)\cos(\varsigma/h) + e(\alpha,\beta)\sin(\varsigma/h)\right]_i$$
$$+ \left[\sum_{k=1}^{n_i} \Psi^k(\alpha,\beta)(\varsigma-\varsigma_k)H_k(\varsigma) + \sum_{k=1}^{n_i} \Omega^k(\alpha,\beta)(\varsigma-\varsigma_k)^2 H_k(\varsigma)\right]_c \quad (22)$$

Like ZZ_NA1, higher-order coefficients are not redefined for each layer, while zig-zag amplitudes are still recomputed by imposing the stress compatibility conditions (16). Because of this, ZZ_NA1 and ZZ_NA2 only partially satisfy the constraints. The results will show that ZZ_NA1 is more accurate than ZZ_NA2. In subsequent sections, authors' previously developed theories and used for comparison in the numerical applications are briefly reviewed.

2.5. HWZZ mixed theory

Displacements of HWZZ [24] derive from those of ZZA neglecting the contributions of Ω^k, which brings usually smaller contributions than Φ_α^k, Ψ^k, which however are not negligible from the standpoint of the slope change at interfaces. Higher-order and adaptive contributions $A_{\alpha 4}\varsigma^4 + \cdots + A_{\alpha n}\varsigma^n$, $A_{\varsigma 5}\varsigma^5 + \cdots + A_{\varsigma n}\varsigma^n$ are also neglected from displacement fields and no decomposition into mathematical layers is allowed, i.e. contributions by $_\alpha C_u^j$, C_ς^j are omitted, so a single-layer zig-zag representation is adopted for displacements.

Out-of-plane strains are constructed assuming the representation (11) by ZZA, while in-plane strains are derived from kinematics [24]. Membrane stresses $\sigma_{\alpha\alpha}$, $\sigma_{\beta\beta}$, $\sigma_{\alpha\beta}$ are obtained in a straightforward way from stress-strain relations. Expressions of out-of-plane stresses are obtained from expressions of membrane stresses by integrating local equilibrium equations. In this way, stress jumps resulting from omission of contributions by Ω^k are recovered and it is prevented that displacement and stress fields fit their counterparts from kinematic assumptions, yielding to no improvements.

2.6. HWZZM adaptive theory with modified Murakami's zig-zag functions

This theory, retaken from [29], is a HW mixed theory where $[...]_0$ and $[...]_i$ are the same as ZZA (11), but different layerwise functions $[...]_c$ are assumed. Layewise contributions to in-plane displacements and the first contribution of the transverse displacement are the same of Murakami's based theories except that a multiplier coefficient is applied constituting the zig-zag amplitude, whose expression is determined by enforcing the compatibility of out-of-plane shear and normal stresses at material layer interfaces. So, differently to Murakami's based models in the literature, layerwise contributions, $[...]_c$ have amplitudes no longer assumed a priori and no longer uniform across the thickness. An additional contribution is incorporated in the transverse displacement, which involves second order powers of ς, whose amplitude is determined by enforcing the continuity of the transverse normal stress gradient. Membrane stresses are obtained from stress-strain relations and used to compute out-of-plane master stresses by integrating local equilibrium equations.

Table 4

Normalized zig-zag amplitudes of theories of section 2.6.1 (normalization factor $(L_\alpha/h) \, p^0$).

Zig-zag amplitudes of theories HWZZM($\square$)

Case	HWZZMA[1]	HWZZMB[1]	HWZZMC[1]	HWZZMB2[u]	HWZZMC2[u]	HWZZM0[1+]
d	$A_k^{u_\alpha} = 0.8921 \cdot 10^{-3}$	$A_k^{u_\alpha} = §$	$A_k^{u_\alpha} = §$	$A_k^{u_\alpha} = §$	$A_k^{u_\alpha} = §$	$A_k^{u_\alpha} = §$
	$A_k^{u_\varsigma} = 0.01269 \cdot 10^{-3}$	$A_k^{u_\varsigma} = 0.01269 \cdot 10^{-3}$	$A_k^{u_\varsigma} = §$	$A_k^{u_\varsigma} = 0.20032 \cdot 10^{-3}$	$A_k^{u_\varsigma} = §$	$A_k^{u_\varsigma} = 0.01269 \cdot 10^{-3}$
	$B_k^{u_\varsigma} = -0.06582 \cdot 10^{-3}$	$B_k^{u_\varsigma} = -0.06582 \cdot 10^{-3}$	$B_k^{u_\varsigma} = -0.06582 \cdot 10^{-3}$	$B_k^{u_\varsigma} = -0.31043 \cdot 10^{-3}$	$B_k^{u_\varsigma} = -0.31043 \cdot 10^{-3}$	$B_k^{u_\varsigma} = 0$
e	$A_k^{u_\alpha} = 0.03639 \cdot 10^{-7}$	$A_k^{u_\alpha} = §$	$A_k^{u_\alpha} = §$	$A_k^{u_\alpha} = §$	$A_k^{u_\alpha} = §$	$A_k^{u_\alpha} = §$
	$A_k^{u_\beta} = 0.01212 \cdot 10^{-7}$	$A_k^{u_\beta} = §$	$A_k^{u_\beta} = §$	$A_k^{u_\beta} = §$	$A_k^{u_\beta} = §$	$A_k^{u_\beta} = §$
	$A_k^{u_\varsigma} = 0.12099 \cdot 10^{-7}$	$A_k^{u_\varsigma} = 0.12099 \cdot 10^{-7}$	$A_k^{u_\varsigma} = §$	$A_k^{u_\varsigma} = 0.00470 \cdot 10^{-7}$	$A_k^{u_\varsigma} = §$	$A_k^{u_\varsigma} = 0.12099 \cdot 10^{-7}$
	$B_k^{u_\varsigma} = 0.00463 \cdot 10^{-7}$	$B_k^{u_\varsigma} = 0.00463 \cdot 10^{-7}$	$B_k^{u_\varsigma} = 0.00463 \cdot 10^{-7}$	$B_k^{u_\varsigma} = -0.00285 \cdot 10^{-7}$	$B_k^{u_\varsigma} = -0.00285 \cdot 10^{-7}$	$B_k^{u_\varsigma} = 0$
f	$A_k^{u_\alpha} = 1.647226 \cdot 10^{3}$	$A_k^{u_\alpha} = §$	$A_k^{u_\alpha} = §$	$A_k^{u_\alpha} = §$	$A_k^{u_\alpha} = §$	$A_k^{u_\alpha} = §$
	$A_k^{u_\varsigma} = -7.02909 \cdot 10^{3}$	$A_k^{u_\varsigma} = -7.02909 \cdot 10^{3}$	$A_k^{u_\varsigma} = §$	$A_k^{u_\varsigma} = -0.403358 \cdot 10^{3}$	$A_k^{u_\varsigma} = §$	$A_k^{u_\varsigma} = -7.02909 \cdot 10^{3}$
	$B_k^{u_\varsigma} = -0.07080 \cdot 10^{3}$	$B_k^{u_\varsigma} = -0.07080 \cdot 10^{3}$	$B_k^{u_\varsigma} = -0.07080 \cdot 10^{3}$	$B_k^{u_\varsigma} = 0.003285 \cdot 10^{3}$	$B_k^{u_\varsigma} = 0.003285 \cdot 10^{3}$	$B_k^{u_\varsigma} = 0$
g	$A_k^{u_\alpha} = 0.662353 \cdot 10^{5}$	$A_k^{u_\alpha} = §$	$A_k^{u_\alpha} = §$	$A_k^{u_\alpha} = §$	$A_k^{u_\alpha} = §$	$A_k^{u_\alpha} = §$
	$A_k^{u_\varsigma} = -0.37616 \cdot 10^{5}$	$A_k^{u_\varsigma} = -0.37616 \cdot 10^{5}$	$A_k^{u_\varsigma} = §$	$A_k^{u_\varsigma} = 0.00094 \cdot 10^{5}$	$A_k^{u_\varsigma} = §$	$A_k^{u_\varsigma} = -0.37616 \cdot 10^{5}$
	$B_k^{u_\varsigma} = 0.010866 \cdot 10^{5}$	$B_k^{u_\varsigma} = 0.010866 \cdot 10^{5}$	$B_k^{u_\varsigma} = 0.010866 \cdot 10^{5}$	$B_k^{u_\varsigma} = -0.00018 \cdot 10^{5}$	$B_k^{u_\varsigma} = -0.00018 \cdot 10^{5}$	$B_k^{u_\varsigma} = 0$
h	$A_k^{u_\alpha} = -227.35774$	$A_k^{u_\alpha} = §$	$A_k^{u_\alpha} = §$	$A_k^{u_\alpha} = §$	$A_k^{u_\alpha} = §$	$A_k^{u_\alpha} = §$
	$A_k^{u_\varsigma} = -11.57605$	$A_k^{u_\varsigma} = -11.57605$	$A_k^{u_\varsigma} = §$	$A_k^{u_\varsigma} = 96.06635$	$A_k^{u_\varsigma} = §$	$A_k^{u_\varsigma} = -11.57605$
	$B_k^{u_\varsigma} = -0.13431$	$B_k^{u_\varsigma} = -0.13431$	$B_k^{u_\varsigma} = -0.13431$	$B_k^{u_\varsigma} = -0.428702$	$B_k^{u_\varsigma} = -0.428702$	$B_k^{u_\varsigma} = 0$
i	$A_k^{u_\alpha} = 0.509847$	$A_k^{u_\alpha} = §$	$A_k^{u_\alpha} = §$	$A_k^{u_\alpha} = §$	$A_k^{u_\alpha} = §$	$A_k^{u_\alpha} = §$
	$A_k^{u_\beta} = -2.681337$	$A_k^{u_\beta} = §$	$A_k^{u_\beta} = §$	$A_k^{u_\beta} = §$	$A_k^{u_\beta} = §$	$A_k^{u_\beta} = §$
	$A_k^{u_\varsigma} = -0.091129$	$A_k^{u_\varsigma} = -0.091129$	$A_k^{u_\varsigma} = §$	$A_k^{u_\varsigma} = 0.011820$	$A_k^{u_\varsigma} = §$	$A_k^{u_\varsigma} = -0.091129$
	$B_k^{u_\varsigma} = 0.0426823$	$B_k^{u_\varsigma} = 0.0426823$	$B_k^{u_\varsigma} = 0.0426823$	$B_k^{u_\varsigma} = -0.006574$	$B_k^{u_\varsigma} = -0.006574$	$B_k^{u_\varsigma} = 0$
j	$A_k^{u_\alpha} = -0.000328$	$A_k^{u_\alpha} = §$	$A_k^{u_\alpha} = §$	$A_k^{u_\alpha} = §$	$A_k^{u_\alpha} = §$	$A_k^{u_\alpha} = §$
	$A_k^{u_\beta} = 0.0000294$	$A_k^{u_\beta} = §$	$A_k^{u_\beta} = §$	$A_k^{u_\beta} = §$	$A_k^{u_\beta} = §$	$A_k^{u_\beta} = §$
	$A_k^{u_\varsigma} = -0.030146$	$A_k^{u_\varsigma} = -0.030146$	$A_k^{u_\varsigma} = §$	$A_k^{u_\varsigma} = 0.031073$	$A_k^{u_\varsigma} = §$	$A_k^{u_\varsigma} = -0.030146$
	$B_k^{u_\varsigma} = -0.048351$	$B_k^{u_\varsigma} = -0.048351$	$B_k^{u_\varsigma} = -0.048351$	$B_k^{u_\varsigma} = -0.047001$	$B_k^{u_\varsigma} = -0.047001$	$B_k^{u_\varsigma} = 0$
k	$A_k^{u_\alpha} = 3.23840$	$A_k^{u_\alpha} = §$	$A_k^{u_\alpha} = §$	$A_k^{u_\alpha} = §$	$A_k^{u_\alpha} = §$	$A_k^{u_\alpha} = §$
	$A_k^{u_\beta} = 3.463523$	$A_k^{u_\beta} = §$	$A_k^{u_\beta} = §$	$A_k^{u_\beta} = §$	$A_k^{u_\beta} = §$	$A_k^{u_\beta} = §$
	$A_k^{u_\varsigma} = 0.033849$	$A_k^{u_\varsigma} = 0.033849$	$A_k^{u_\varsigma} = §$	$A_k^{u_\varsigma} = 0.077460$	$A_k^{u_\varsigma} = 0.077460$	$A_k^{u_\varsigma} = 0.033849$
	$B_k^{u_\varsigma} = -0.002361$	$B_k^{u_\varsigma} = -0.002361$	$B_k^{u_\varsigma} = -0.002361$	$B_k^{u_\varsigma} = -0.001113$	$B_k^{u_\varsigma} = §$	$B_k^{u_\varsigma} = 0$

§: zig-zag amplitudes are calculated as indicated in sect. 2.6.1.

[u] Zig-zag amplitudes are assumed coincident with those at the first interface from above.

[1] Zig-zag amplitudes are assumed coincident with those at the first interface from below.

[+] Zig-zag amplitudes $B_k^{u_\varsigma}$ are assumed null.

The purpose of this theory is to test whether results with the same accuracy of ZZA and HWZZ can be effectively obtained although zig-zag functions are chosen in a different way.

Modified versions of HWZZM are also considered whose amplitudes of zig-zag functions are assumed and then are kept uniform across the thickness (see Table 4), in order to clarify the importance of the redefinition of coefficients on accuracy.

2.6.1. Murakami's like theories

Theories HWZZMA, HWZZMB, HWZZMC, HWZZMB2, HWZZMC2 and HWZZM0 are derived from HWZZM as outlined forward.

– $A_k^{u_\alpha}(\varsigma)$, $A_k^{u_\varsigma}(\varsigma)$ and $B_k^{u_\varsigma}(\varsigma)$ of HWZZMA are assumed uniform and coincident with those of HWZZM at the first interface from below. $A_k^{u_\alpha}(\varsigma)$, and $B_k^{u_\varsigma}(\varsigma)$ of HWZZMB are assumed like in HWZZMA while $A_k^{u_\varsigma}(\varsigma)$ is calculated like in HWZZM theory.

– For HWZZMC, only $B_k^{u_\varsigma}(\varsigma)$ amplitudes are assumed uniform across the thickness and coincident with those at the first interface from below. $B_k^{u_\varsigma}(\varsigma)$ contributions are neglected for HWZZM0, while $A_k^{u_\alpha}(\varsigma)$, $A_k^{u_\varsigma}(\varsigma)$ are assumed in the same way of HWZZMB.

– HWZZMB2 and HWZZMC2 theories are similar to HWZZMB and HWZZMC, respectively, but currently amplitudes are assumed coincident with those of HWZZM at the first interface from above. With the exception of the parameters explicitly indicated, all the rest remains the same as HWZZM.

However, since the amplitudes are not redefined, the results will show that accuracy is lost, therefore they are not convenient even though a processing time saving by 10% is obtained.

Anticipating the numerical findings, the most accurate theories of this group will prove to be ZZA, ZZA1, ZZA2, ZZA3, HWZZ and HWZZM, being the only ones able to achieve results comparable to those of FEA 3-D for all the examined cases. Because the zig-zag functions of HWZZM differ from those of ZZA and HWZZ when, in fact, their results are indistinguishable, there is evidence that the choice of such functions is immaterial.

3. Lower-order theories

Lower-order theories in HW and HR forms are considered in the numerical assessments, which assume either a uniform or a polynomial description of the transverse displacement. They are considered for assessing whether and for which application they can be as accurate as their higher-order counterparts of section 2.

3.1. MHR, MHR±, MHRO theories

A cubic-quartic mixed zig-zag theory referred as MHR [24], is considered for comparisons which just incorporates Murakami's zig-zag function $M^k(\varsigma)$ as the layerwise function within in-plane displacements:

$$u_\alpha(\alpha, \beta, \varsigma) = \left[u_\alpha^0(\alpha, \beta) + \varsigma\left(\Gamma_\alpha^0(\alpha, \beta) - w^0(\alpha, \beta),_\alpha\right)\right]_0 + \left[C_\alpha(\alpha, \beta)\varsigma^2 + D_\alpha(\alpha, \beta)\varsigma^3\right]_i + E_\alpha(\alpha, \beta)M^k(\varsigma) \tag{23}$$

$$u_\varsigma(\alpha, \beta, \varsigma) = \left[w^0(\alpha, \beta)\right]_0 + \left[a(\alpha, \beta)\varsigma + b(\alpha, \beta)\varsigma^2 + c(\alpha, \beta)\varsigma^3 + d(\alpha, \beta)\varsigma^4\right]_i$$

Coefficients C_α, D_α, a, b, c, d are calculated by enforcing the fulfillment of stress boundaries conditions (14), while terms E_α are calculated by enforcing the fulfillment of first and second equilibrium equations (15) at the middle-plane of the laminate. In this case, a unique computational layer is assumed across the whole laminate thickness. Because transverse shear and normal stresses cannot be continuous at layer interfaces due to the assumptions made, their expressions within the framework of HR variational theorem (2) must be obtained integrating local equilibrium equations.

A refined version of MHR, here referred as MHR± is retaken from [29] where the sign of Murakami's zig-zag function is determined on a physical basis, instead of being forced to reverse at interfaces. The correct slope sign is determined at each interface comparing whether out-of-plane stresses are more accurate assuming a positive or a negative slope, namely which choice produces the lowest norm of the residual force from the three local equilibrium equations.

Another new theory referred as MHRO is considered, whose displacement field is the same of (24) but E_α are assumed as an additional d.o.f. Results by MHRO will be only provided for case d, as an example just to show that, despite an additional d.o.f. is considered, no advantage is achieved because the same accuracy of MHR is obtained.

3.2. MHR4, MHWZZA, MHWZZA4 and MHR4± theories

The following theories derived from MHR are further considered for comparison purposes. Theory MHR4 [24] is derived assuming the following fourth-order through-thickness piecewise variation of the transverse displacement:

$$u_\varsigma(\alpha, \beta, \varsigma) = \left[w^0(\alpha, \beta)\right]_0 + \left[a(\alpha, \beta)\varsigma + b(\alpha, \beta)\varsigma^2 + c(\alpha, \beta)\varsigma^3 + d(\alpha, \beta)\varsigma^4\right]_i + e(\alpha, \beta)M^k(\varsigma) \tag{24}$$

In this case, e is calculated by enforcing the fulfillment of the third local equilibrium equation at the middle-plane.

A supplementary version of MHR indicated as MHWZZA [24] is considered, which was developed from the HW theorem assuming as master displacement-field the same of MHR, the same master strain and master stress fields of HWZZ. In an attempt of improving accuracy, ZZA is used as the post-processor.

Another theory used for comparison purposes is MHWZZA4 [24], which was derived from the HW variational statement assuming the in-plane displacements by MHR, the transverse displacement by ZZA and as master strain and stress fields those of the HWZZ model. So, the only substantial difference of MHWZZA and MHWZZA4 with respect to HWZZ and ZZA is the use of Murakami's like instead of Di Sciuva's like zig-zag function within a simplified displacement field.

Finally, theory MHR4± derived from MHR4 is considered, where similarly to MHR± the sign of Murakami's zig-zag function is determined on a physical basis following the same process described in section 3.1.

3.3. HRZZ and HRZZ4 theory

Another lower order theory used in the numerical applications for comparison purposes is HRZZ [24], which was developed from the HR statement (2) postulating a uniform transverse displacement and a cubic zig-zag representation of in-plane displacements:

$$u_\alpha(\alpha, \beta, \varsigma) = \left[u_\alpha^0(\alpha, \beta) + \varsigma\left(\Gamma_\alpha^0(\alpha, \beta) - w^0(\alpha, \beta),_\alpha\right)\right]_0 + \left[C_\alpha^i(\alpha, \beta)\varsigma^2 + D_\alpha^i(\alpha, \beta)\varsigma^3\right]_i$$

$$+ \left[\sum_{k=1}^{n_i} \Phi_\alpha^k(\alpha, \beta)(\varsigma - \varsigma_k)H_k(\varsigma) + \sum_{k=1}^{3} {}_\alpha C_u^k(\alpha, \beta)H_k(\varsigma)\right]_c \tag{25}$$

$$u_\varsigma(\alpha, \beta, \varsigma) = w^0(\alpha, \beta)$$

The transverse normal stress σ_{33} is assumed the same of ZZA model, while transverse shear stresses σ_{i3} are derived from equilibrium equations starting from membrane stresses obtained from kinematics. A version of HRZZ indicated as HRZZ PP is particularized, wherein the ZZA model is used as the post-processor in order to improve accuracy.

Another theory HRZZ4 is considered for comparison purposes, which assumes a fourth-order polynomial approximation of the transverse displacement as:

$$u_\varsigma(\alpha, \beta, \varsigma) = \left[w^0(\alpha, \beta)\right]_0 + \left[b(\alpha, \beta)\varsigma + c(\alpha, \beta)\varsigma^2 + d(\alpha, \beta)\varsigma^3 + e(\alpha, \beta)\varsigma^4\right]_i \tag{26}$$

and the same stress field of HRZZ (note that ε_{33}^u is no longer null as in HRZZ). This latter theory is aimed at improving accuracy of HRZZ when the properties of constituent layers largely vary across the thickness.

Table 5

Mechanical properties considered in numerical applications.

Elastic moduli	Material name												
	c1 [iso]	c2 [iso]	i1	i2	mc	n [iso]	p	q	r	s1	s2	s3	s4
E1 [GPa]	–	–	6.89	0.1	0.1	–	172.4	0.273	25E2	1	33	25	0.05
E2 [GPa]	–	–	6.89	0.1	0.1	–	6.89	0.273	E2	1	1	1	0.05
E3 [GPa]	M1	M2	6.89	0.1	0.1	M3	6.89	0.273	E2	1	1	1	0.05
G12 [GPa]	–	–	2.59	0.037	0.04	–	3.45	0.1102	0.5E2	0.2	0.8	0.5	0.0217
G13 [GPa]	–	–	2.59	0.037	0.04	–	3.45	0.413	0.5E2	0.2	0.8	0.5	0.0217
G23 [GPa]	–	–	2.59	0.037	0.04	–	1.378	0.413	0.2E2	0.2	0.8	0.5	0.0217
$\upsilon12$	0.34	0.34	0.33	0.33	0.25	0.33	0.25	0.25	0.25	0.25	0.25	0.25	0.15
$\upsilon13$	0.34	0.34	0.33	0.33	0.25	0.33	0.25	0.25	0.25	0.25	0.25	0.25	0.15
$\upsilon23$	0.34	0.34	0.33	0.33	0.25	0.33	0.25	0.25	0.25	0.25	0.25	0.25	0.15

M1 $E_l/E_u = 5/4$, $E_l/E_c = 10^5$ M2 $E_l/E_u = 5/4$, $E_l/E_c = 10^4$ M3 $E_u/E_l = 1.6$, $E_u/E_c = 166.66$ [iso] = isotropic $E_1 = E_2 = E_3$ $G_1 = G_2 = G_3$

Table 6

Processing time [s], including symbolic computations. Calculations made by a laptop computer with quad-core CPU @ 2.60 GHz, 64-bit operating system and 8.00 GB RAM.

	Case	Cases							
		d	e	f	g	h	i	h	k
Adaptive theories	ZZA	13.5620	10.6297	15.0671	15.9719	15.0671	10.5392	10.3465	10.9591
	ZZA1	10.9875	6.0213	10.4752	10.8763	10.6351	5.5423	5.9752	5.9741
	ZZA2	10.9742	6.0317	10.485	10.8564	10.6241	5.6574	5.8741	6.0244
	ZZA3	10.9657	6.0417	10.4784	10.7419	10.5934	5.5479	5.5369	5.7465
	HWZZ	12.0193	6.6997	12.4271	12.8490	12.4271	6.4675	6.5745	6.7755
	HWZZM	11.0702	6.1781	11.5344	11.7059	11.5359	5.9675	6.1899	6.2402
HR theories	HRZZ	14.9182	11.6926	18.2312	18.2261	18.2312	11.5234	11.6618	12.5887
	HRZZ PP	17.1412	13.5781	18.8624	18.1405	18.8624	13.4823	12.0989	13.3635
	HRZZ4	14.7821	11.6649	18.2237	18.4891	18.2237	11.8083	11.4963	12.5681
	MHR	8.1514	6.5659	6.9574	6.6258	6.9574	6.7454	6.8583	6.6732
	MHR4	8.6564	6.4724	6.4946	6.9702	6.4946	6.5908	6.2430	6.5056
HW theories	MHWZZA	10.7396	8.2006	7.2359	7.6952	7.2359	8.2660	8.3921	8.6730
	MHWZZA4	10.2451	8.6045	7.8365	7.5861	7.8365	8.5094	8.0087	8.9862
	HWZZMA	10.9925	6.1642	11.5265	11.6018	11.5267	5.9249	6.0498	6.0951
	HWZZMB	11.0215	6.1737	11.5307	11.6289	11.5317	5.9423	6.1003	6.1143
	HWZZMC	11.0498	6.1772	11.5314	11.6457	11.5326	5.9543	6.1240	6.1597
	HWZZMB2	11.0314	6.1737	11.5310	11.6389	11.5301	5.9472	6.1157	6.1142
	HWZZMC2	11.0492	6.1772	11.5317	11.6401	11.5334	5.9498	6.1291	6.1457
	HWZZM0	10.9611	6.0856	11.4287	11.5912	11.4873	5.8752	6.0327	6.0475

4. Numerical assessments and discussion

The accuracy of previous theories is assessed considering challenging benchmarks with strong layerwise effects resulting from elastic properties, lay-up, loading and boundary conditions.

Benchmarks a to g and i to k are retaken from [24,29], while h is considered for the first time in this paper. Throughout the body of numerical results, the reference solutions consist of exact results, whenever available, or FEA 3-D results [50].

Material properties, lay-up, loading and boundary conditions, trial functions, expansion order, FEA-3D meshing, normalizations and length-to-thickness ratios considered are reported in Tables 2, 3 and 5 respectively. Symbols *, □ and § of Table 2 indicate when Murakami's slope rule fails for displacements u_α, u_β or u_ς. Positions where displacements and stresses are reported are explicitly defined in Table 3. The processing time required to carry out computation for each case examined is reported in Table 6. It comprises post-processing operations carried out for recovering stresses, in the cases where they are applied. In all cases examined, the number of equilibrium points considered is equal to $\Im_l \cdot (n_u - 1) - 2$, where $\Im_l$ is the number of computational or physical layers and n_u is the expansion order of the in-plane displacement, (in this paper $n_u = 3$).

4.1. Preliminary tests a to c for assessing the correct implementation of theories

Results of these cases are reported in Tables 7a to 7c. In addition to verify the correct implementation of theories, they also serve to ascertain whether there can be a certain diversification of predictions of theories, despite these cases are not particularly demanding.

Displacements and stresses of case a [51] (Table 7a) obtained by "adaptive" theories HWZZ, HWZZM, ZZA1, ZZA2, ZZA3 and ZZA whose coefficients are redefined across the thickness prove to be indistinguishable from each other and very close to exact solution.

So it starts to be already demonstrated that the choice of zig-zag functions is immaterial and they can be changed or omitted without any loss of accuracy. The results by ZZA3 also starts demonstrating that other functions than power series can be used within adaptive theories in order to represent the transverse variation of displacements, without any loss of precision. For this reason from now on, the results of adaptive theories will be merged in Figures and Tables. Anyway it should be noticed that present theories obtain very accurate results with only five d.o.f., unlike non-physically-based theories in literature. The results reported in Table 7b for case b [22] confirm what previously stated, while the results for case c require a detailed discussion. Such case, which is retaken from [19], refers to a sandwich beam with a transversely soft lower face (E_3 reduced by a factor of 10^{-2}), which is simulated as an eleven layers laminate (five for each face and one for the core). Transverse shear stress assume an opposite sign across the faces, which is a very interesting and challenging feature to capture. The results for this case reported in Table 7c confirm the absolute equivalence of the adaptive theories and that the

Table 7a

Displacements and stresses for the case a. Position is that across the thickness measured from the middle plane (the same applies to the following Tables 7b to 9g).

Case a		Exact [51]	FEA 3-D	ZZA	ZZA1	ZZA2	ZZA3	HWZZ	HWZZM
					Theories				
u_α	$-h/2$	3.6968	3.6823	3.6944	3.6944	3.6944	3.6946	3.6944	3.6944
u_ς	0	7.2069	7.2170	7.1981	7.1981	7.1981	7.1985	7.1981	7.1981
$\sigma_{\alpha\alpha}$	$-h/2$	-58.1420	-58.8002	-58.7972	-58.7972	-58.7972	-58.8026	-58.7972	-58.7972
$\sigma_{\alpha\varsigma}$	0	1.9533	1.9588	1.9521	1.9521	1.9521	1.9522	1.9521	1.9521

Table 7b

Displacements and stresses for the case b.

Case b		[22]	FEA 3-D	ZZA	ZZA1	ZZA2	ZZA3	HWZZ	HWZZM
					Theories				
u_α	$-h/2$	4.5502	4.5539	4.5522	4.5522	4.5522	4.5523	4.5522	4.5522
u_ς	0	4.6952	4.6964	4.6888	4.6888	4.6888	4.6892	4.6888	4.6888
$\sigma_{\alpha\alpha}$	$h/2$	30.0280	30.3910	30.3508	30.3508	30.3508	30.3524	30.3508	30.3508
	$-h/2$	-3.8358	-3.8453	-3.8374	-3.8374	-3.8374	-3.8376	-3.8374	-3.8374
$\sigma_{\alpha\varsigma}$	$h/4$	2.7061	2.6843	2.7067	2.7067	2.7067	2.7069	2.7067	2.7067

Table 7c

Displacements and stresses for the case c.

Case c		FEA 3-D	ZZA	ZZA1	ZZA2	ZZA3	HWZZ	HWZZM	ZZ_NA1	ZZ_NA2
						Theories				
u_α	up	-0.0153	-0.0153	-0.0153	-0.0153	-0.0153	-0.0153	-0.0153	-0.0251	-0.0273
	down	-0.0026	-0.0026	-0.0026	-0.0026	-0.0026	-0.0026	-0.0026	-0.0107	-0.0130
	max	0.0424	0.0426	0.0426	0.0426	0.0426	0.0426	0.0426	0.0312	0.0718
	min	-0.0153	-0.0152	-0.0152	-0.0152	-0.0152	-0.0152	-0.0152	-0.0251	-0.0273
u_ς	up/max	0.3861	0.3864	0.3864	0.3864	0.3864	0.3864	0.3864	0.6208	0.6625
	down	-0.0875	-0.0872	-0.0872	-0.0872	-0.0872	-0.0872	-0.0872	-0.2919	-0.3403
	min	-0.0876	-0.0878	-0.0878	-0.0878	-0.0878	-0.0878	-0.0878	-0.2920	-0.3404
$\sigma_{\alpha\alpha}$	up	0.8734	0.8732	0.8732	0.8732	0.8732	0.8732	0.8732	1.3344	1.4512
	down	0.1448	0.1453	0.1453	0.1453	0.1453	0.1453	0.1453	0.5586	0.6795
	max	21.4108	21.4011	21.4011	21.4011	21.4011	21.4011	21.4011	32.8438	35.9172
	min	-16.4857	-16.4760	-16.4760	-16.4760	-16.4760	-16.4760	-16.4760	-27.0462	-29.1637
$\sigma_{\alpha\varsigma}$	max	5.7005	5.7337	5.7337	5.7337	5.7337	5.7337	5.7337	8.4452	9.4429
	min	-0.6490	-0.6512	-0.6512	-0.6512	-0.6512	-0.6512	-0.6512	-3.1219	-3.9930
$\sigma_{\varsigma\varsigma}$	up/max	1.0000	1.0000	1.0000	1.0000	1.0000	1.0000	1.0000	1.0000	1.0000
	min	-0.0252	-0.0252	-0.0252	-0.0252	-0.0252	-0.0252	-0.0252	-0.1523	-0.1817

choice of representation and zig-zag functions is immaterial. Vice-versa, the accuracy of the theories that impose only a partial set of physical constraints results to be largely dependent upon their choices and highly susceptible to the variation of layer thickness and elastic properties assumed.

This becomes evident by comparing the results by non-adaptive theories ZZ_NA1 and ZZ_NA2, where only zig-zag amplitudes are recomputed across the thickness. Indeed, the first one, that assume a polynomial representation, shows a superior accuracy than its counterpart ZZ_NA2, which uses a combination of sinusoidal, power and exponential functions across the thickness. However, because only a partial set of physical constraints is imposed, precision of adaptive theories cannot be obtained, so, their results won't be reported in the following much challenging cases for sake of brevity.

In all cases a to c, the superior efficiency of adaptive theories ZZA, ZZA1, ZZA2, ZZA3, HWZZ and HWZZM is clearly shown by the processing time reported in Table 6.

4.2. Case d – cross play laminated beam

A simply supported $[0/-90/0/-90]$ laminated beam in cylindrical bending under sinusoidal loading is now considered. Retaken from [52] and [53], this case is interesting because strong layerwise effects rise as a result of the stacking. Henceforth Tables will show the quantities that are not shown in the figures (if any), in order not to present redundant data. In Tables 8a to 8h reporting the results for this case, as also forward for the remaining ones, theories MHR, MHR4, MHR± and MHR4± are merged (♦) for sake of brevity if not explicitly reported, because their results differ by only 3% to 8% each other. In this and following cases, the results of the theories ZZA, ZZA1, ZZA2, ZZA3, HWZZ, HWZZM (♠) are grouped together, as their results are practically coincident. This fact must be understood as the demonstration that the choice of the representation and zig-zag functions is immaterial for adaptive theories of sections 2.4 to 2.6.

The effects of support reactions is shown in Tables 9a to 9g. To consider this effect, a transverse normal stress $\sigma_{\varsigma\varsigma}$ (with the magnitude specified case by case) is applied at a distance less that 1% of the length away from the supports, because the trigonometric trial functions identically vanish at the supports.

Results show that a periodical stack-up not necessarily implies a slope sign reversal at interfaces, contrary to what postulated by Murakami's zig-zag function. Furthermore it is noted that only adaptive theories can accurately predict u_α and $\sigma_{\alpha\varsigma}$, while all theories (except MHR, MHR4, MHWZZA and MHWZZA4 at the first interface from above) quite accurately capture $\sigma_{\alpha\alpha}$, $\sigma_{\varsigma\varsigma}$ and u_ς. Anyway, major

errors are committed by HWZZMB and HWZZM0, while MHRO prove in this case to be as accurate as MHR, therefore it doesn't benefit from the extra d.o.f. Results by MHR± and MHR4± show no improvement as regards the accuracy of the transverse displacement, which appears the most difficult quantity to determine. HRZZ can't even predict the average value of this displacement also when post-processed by ZZA (results indicated as HRZZ PP).

As regard the effects of supports, (in this case the application of $\sigma_{\varsigma\varsigma}^{-} = -0.1p_0^u$), Table 9a shows that an inappreciable variation of u_α is induced across the thickness, but despite this, the errors committed by lower-order and Murakami's based theories increases. Instead, the effects of support reactions on transverse normal stress is predicted with an excellent agreement by all theories, accordingly is not reported.

Adaptive theories ZZA, ZZA1, ZZA2, ZZA3, HWZZ and HWZZM again prove to be the most efficient ones as shown in Table 6. It is noted that simplified theories based on Hellinger-Reissner and Hu-Washizu variational theorem neither are accurate, nor can save overall costs in this case.

4.3. Case e – simply supported rectangular sandwich plate

A simply supported rectangular sandwich plate under bi-sinusoidal loading is retaken from Brischetto et al. [25], since strong layerwise effects rise due to the stiffer and thinner lower face. In this case, the slope of in-plane displacements reverses at the lower interface as postulated by Murakami's zig-zag function, but not at the upper one. This explains why the errors made by plate theories using Murakami's zig-zag function grow up from the bottom to top, as shown in Table 8b. For compensating such errors, a higher degree of expansion of the variables would be required (e.g., over the 7-th order [25]). However, it should be noted that the low expansion order used for all theories allows adaptive theories to provide already very accurate results.

In details, the results of Table 8b show that no advantages are gotten in this case by MHR± which determined the right slope sign because of its still too poor kinematics. Owing to less limiting kinematic assumptions, MHR4 gets better transverse shear stresses than MHR4±.

As in all previous cases, adaptive theories achieve the best results and always in perfect agreement with each other, demonstrating again that the choice of representation and zig-zag functions is immaterial for them and that the latter can even be explicitly omitted without any accuracy loss.

In this case, also all theories with a priori assumed zig-zag functions that are not redefined through imposition of constraints, prove to be fairly accurate. However ones of lower order appear inaccurate at some point across the thickness.

All lower order theories using Murakami's zig-zag function provide an incorrect prediction after the first interface from below (Fig. 1 and Table 9b) when the effects of constraint stresses are considered ($\sigma_{\varsigma\varsigma}^{-} = -0.1p_0^u$ at supported edges). Moreover, results by theories HWZZMA, HRZZ, HRZZ PP, HRZZA4 and MHR and MHR4 are not reported for this case, being too inaccurate.

Also in this case, adaptive theories ZZA1, ZZA2, ZZA3, HWZZ and HWZZM prove to be the most efficient ones (see Table 6).

4.4. Cases f, g and h – Propped cantilever sandwich beams

Currently, a propped-cantilever sandwich beam (clamped at $\alpha = 0$ and restrained on the lower face at $\alpha = L_\alpha$) [24,47] is considered, which is loaded by a uniform transverse distributed loading on the upper face. Lower $_{(l)}$ and upper $^{(u)}$ faces are assumed to be $t_l = c/2$ and $t_u = c/4$ thick, respectively, c being the thickness of core. The following ratios of elastic moduli of faces $E_u/E_l = 1.6$ and core $E_u/E_c = 166.6$ are assumed (all constituent materials have a Poisson's ratio $\upsilon = 0.3$). Initially, the length-to-thickness ratios $L_\alpha/h = 5.714$ is considered (case f), than a ratio of 20 (case g). Subsequently, the position of the support is moved to $\alpha = 0.9L_\alpha$ with $L_\alpha/h = 5.714$ (case h). The peculiar characteristic is that for these cases the through-thickness variation of the transverse normal displacement and stress need to be very accurately reproduced at the restrained edge, otherwise a wrong transverse shear stress field is predicted. Like for case c, another challenging feature is that the transverse shear stress assumes an opposite sign across upper and lower faces at the supported edge. This benchmark is also challenging because at the clamped edge the shear force resultant cannot vanish, as erroneously predicted by many theories in the literature. Add those interesting features up, this benchmark turns out to be a pretty tough case for assessing the accuracy of theoretical models.

4.4.1. Case f

Results by Fig. 2 and Table 8c prove that Murakami's hypothesis is not valuable. As a direct consequence, MHR and MHR4 erroneously predict the through-thickness distribution of displacements and also non-adaptive theories MHWZZA, MHWZZA4, HRZZ, HRZZ PP and HRZZ4 cannot be as accurate as adaptive ones. It could be noticed that results by MHR, MHR4, MHR± and MHR4± differ from each other by only 3% but they make mistakes up to 180% compared to adaptive theories and to FEA 3-D.

The results of ZZA, ZZA1, ZZA2, ZZA3, HWZZ and HWZZM again coincide with each other and are in excellent agreement with FEA 3-D, confirming that the choice of representation and zig-zag functions is immaterial and that even the latter can be omitted if other coefficients can play their role.

Once the effect of the constraint stress are accounted for at the supported edge ($\sigma_{\varsigma\varsigma}^{-} = -5p_0^u$), $\sigma_{\alpha\varsigma}$ considerably decreases across the core and at the lower interface, while constraint stresses have no effects on the in-plane stress distribution (Fig. 3 and Table 9c). It is noted that also for this case lower order theories results show a greater dispersion because an imprecise representation of $\sigma_{\varsigma\varsigma}$ at supports undermines their accuracy.

4.4.2. Case g

Fig. 4 and Table 8d show the result for this case highlighting that $\sigma_{\varsigma\varsigma}$ is strongly asymmetric across the two faces as a consequence of different properties and thickness of faces. It is also noted the inaccuracy of MHWZZA and MHWZZA4 compared to adaptive theories ZZA, ZZA1, ZZA2, ZZA3, HWZZM and HWZZ, which again show all similar results, confirming that the choice of representation and layerwise functions is immaterial for these theories. Anyway, discrepancies are reduced when u_α and $\sigma_{\alpha\varsigma}$ are considered, though lower-order theories remain not very accurate. In this case, MHR, MHR4, MHR± and MHR4± differ again from each other by 3% but they make mistakes up to 90% compared to adaptive theories and to FEA 3-D. The obvious conclusion is that even for a length-to-thickness ratio of

Table 8a
Results for case d; Data ♦ group theories MHR, MHR4, MHR± and MHR4± with errors up to 8%; data ♠ group theories ZZA, ZZA1, ZZA2, ZZA3, HWZZ, HWZZM, which give coincident results; '' means equal.

Case d		FEA 3-D	♠	HRZZ	HRZZ PP	HRZZ4	♦	MHWZZA	MHWZZA4	HWZZMB	HWZZMC	HWZZMB2	HWZZMC2	HWZZM0	MHRO
u_α	up/min	−3.0036	−2.9343	−2.8735	−2.8735	−3.0613	−2.2894	−2.3467	−2.9941	−3.1252	−3.0442	−2.8123	−2.9760	−3.2506	−2.2901
	down/max	1.2439	1.2161	1.2228	1.2228	1.3328	1.3072	1.3399	1.2415	1.2221	1.2733	1.2207	1.2524	1.2460	1.3105
u_ς	up/max	1.6049	1.5955	1.5575	1.6110	1.6030	1.4770	1.5413	1.5792	1.5496	1.6076	1.5407	1.5990	1.5029	1.5139
$\times 10^{-3}$	down	1.5365	1.5281	1.5575	1.5435	1.5355	1.4228	1.4749	1.5129	1.5552	1.5247	1.4341	1.4982	1.5286	1.4596
	min	''	''	''	''	''	''	''	''	1.5254	''	''	''	1.4865	''
$\sigma_{\alpha\alpha}$	up	2.5207	2.5832	2.6382	2.6382	2.6263	2.0558	2.4924	2.5645	2.8471	2.6500	2.4326	2.5963	2.8125	2.2719
	down/min	−24.9701	−24.9931	−25.3961	−25.3961	−25.9016	−25.7320	−24.0193	−25.0093	−25.3803	−25.0854	−23.6711	−24.6739	−24.5472	−28.5263
	max	22.2540	22.3134	22.5404	22.5404	23.2554	21.7952	20.1360	22.8737	26.8990	22.7609	19.8243	21.9048	26.8788	24.1115
$\sigma_{\alpha\alpha}$	up	2.0079	2.0000	2.0297	2.0297	2.0162	2.0150	1.9910	2.0075	2.0011	2.0051	1.9568	1.9988	1.8618	

Table 8b
Results for case e.

Case e		Exact	FEA 3-D	♠	HRZZ	HRZZ PP	HRZZ4	MHR MHR±	MHR4	MHR4±	MHWZZA	MHWZZA4	HWZZMA	HWZZMB	HWZZMC	HWZZMB2	HWZZMC2	HWZZM0
u_α	up/min	−4.0854	−4.0859	−4.0849	−2.6676	−2.6676	−2.6869	−4.1787	−4.1792	−4.8887	−4.1797	−3.5706	−5.3321	−5.3264	−3.9403	−3.5897	−3.9326	−3.5123
$\times 10^{-5}$	down	0.5793	0.5784	0.5791	1.0646	1.0646	0.9874	0.9437	0.9475	0.8194	0.9486	0.2556	0.7189	0.0438	0.5802	1.7524	0.5233	1.8015
	max	8.6280	8.6274	8.6278	7.4391	7.4391	7.4513	6.4477	6.4503	4.2330	6.4568	8.9052	10.6532	9.5517	8.3967	3.6044	8.5372	3.6130
u_β	up/min	–	−0.8757	−0.8761	−0.9438	−0.9438	−0.9219	−0.8634	−0.8617	−0.8148	−0.8213	−0.7981	−1.1893	−1.1837	−0.8756	−0.8739	−0.7977	−0.7806
$\times 10^{-3}$	down	0.1335	0.1335	0.1343	0.3857	0.3857	0.3731	0.4365	0.4339	0.1309	0.0599	0.0599	0.1598	0.0100	0.1279	0.1153	0.3892	0.3999
	max	-	1.8553	1.8569	1.8470	1.8470	1.8265	0.6721	0.6745	0.7055	2.6592	2.2603	2.3652	2.1227	1.8656	1.8968	0.8010	0.8030
u_ς	up	–	0.3362	0.3369	0.1978	0.3631	0.3624	0.1968	0.2170	0.2920	0.3629	0.3657	0.4290	0.3630	0.3368	0.3353	0.3071	0.3042
$\times 10^{-1}$	down/min	–	0.1013	0.1023	0.1978	0.2047	0.2042	0.1985	0.1533	0.2168	0.0039	0.0046	0.1252	0.0701	0.0998	0.0936	0.2973	0.3058
	max	–	0.3368	0.3375	0.1978	0.3640	0.3637	0.1986	0.2174	0.2927	0.3634	0.3661	0.4303	0.3645	0.3374	0.3359	0.3076	0.3059
$\sigma_{\alpha\alpha}$	up/max	–	12.1506	12.1429	13.0801	13.0801	13.1203	11.2863	11.2696	11.7698	13.3864	13.4001	10.4368	13.1275	12.1368	11.0599	12.1132	10.8221
	down	-	−2.3362	−2.3211	−6.6645	−6.6645	−6.6800	−4.5254	−4.5133	−5.8788	−1.0358	−1.2584	−1.7557	0.8542	−2.2272	−6.7292	−2.0089	−6.9174
	min	-	−12.1504	−12.1364	−13.0764	−13.0764	−13.0967	−11.3436	−11.3279	−9.3015	−11.1589	−11.2895	−10.2338	−18.1194	−12.1321	−11.0971	−12.1352	−11.5095
$\sigma_{\beta\beta}$	up/max	–	5.2998	5.2966	5.7040	5.7040	5.6845	4.9606	4.7639	4.9041	4.9677	5.0029	5.2184	5.7076	5.2939	4.8258	5.2837	4.7225
	down	-	−1.0103	−1.0089	−2.8970	−2.8970	−2.8763	−1.9672	−1.7825	−2.4495	−0.4503	−0.4814	−0.8778	0.3714	−0.9666	−2.9247	−0.8717	−3.0062
	min	-	−5.2918	−5.2746	−5.6846	−5.6846	−5.6537	−6.4924	−6.1957	−3.8756	−4.8491	−4.8763	−5.1169	−7.1591	−5.2727	−4.8377	−5.2741	−5.2350
$\sigma_{\alpha\beta}$	up/min	–	−2.5701	−2.5674	−2.7660	−2.7660	−2.7432	−2.3721	−2.3678	−2.4883	−2.4070	−2.3916	−3.4789	−2.2875	−2.5661	−2.3378	−2.5611	−2.4070
	down	-	0.4968	0.4920	1.4128	1.4128	1.3986	0.9594	0.9465	1.2464	0.2196	0.2095	0.5852	1.4657	0.4705	1.4261	0.4242	0.2196
	max	-	2.5765	2.5732	2.7719	2.7719	2.7545	1.8192	1.8192	2.2816	2.3662	2.312	3.4113	2.3530	2.5723	2.3473	2.5729	2.3662
$\sigma_{\alpha\varsigma}$	max	2.0455	2.1140	2.0659	1.8164	1.8164	1.8204	1.9339	2.0878	2.1317	1.8421	2.0502	2.2800	2.4351	2.0541	1.8805	1.9188	1.8787
$\sigma_{\beta\varsigma}$	max	-	2.7185	2.7184	3.0702	3.0702	3.0327	2.5127	2.5925	2.5925	2.5739	2.6105	3.0295	3.2418	2.7363	2.5021	2.5557	2.4766

Table 8c

Results for case f; data ♦ group theories MHR, MHR4, MHR± and MHR4± making similar large errors.

Case f		FEA 3-D	♠	HRZZ HRZZ PP	HRZZ4	♦	MHWZZA	MHWZZA4	HWZZMB	HWZZMC	HWZZMB2	HWZZMC2	HWZZM0
				Theories									
$\sigma_{\alpha\alpha}$	up	−0.5157	−0.5109	−0.3434	−0.3455	0.7151	−0.5038	−0.5046	−0.5314	−0.5247	−0.4701	−0.5314	−0.4884
	down/min	−1.2875	−1.2840	−1.4654	−1.4705	−1.1662	−1.3803	−1.3963	−1.3354	−1.3187	−1.1813	−1.3354	−1.2276
	max	0.9671	0.9681	1.2405	1.2474	0.7151	1.2724	1.2607	1.0068	0.9942	0.8906	1.0068	0.9255

Table 8d

Results for case g; data ♦ group theories MHR, MHR4, MHR± and MHR4± making similar large errors.

Case g		FEA 3-D	♠	HRZZ	HRZZ PP	HRZZ4	♦	MHWZZA	MHWZZA4	HWZZMB	HWZZMC	HWZZMB2	HWZZMC2	HWZZM0
					Theories									
u_ς $\times 10^{-3}$	up	7.7178	7.7177	0	7.4873	7.4874	8.0429	7.6008	7.6008	0.6808	9.1130	1.9626	9.0265	1.9286
	down/min	0	0	0	0	0	0	0	0	−1.5326	0	−0.3168	0	−0.1776
	max	7.7446	7.7499	0	7.4970	7.4934	8.1313	7.6008	7.6203	0.7067	9.1408	1.9868	9.0541	1.9774
$\sigma_{\alpha\alpha}$	up	0.1357	0.1348	0.1106	0.1106	0.1061	0.2579	0.2903	0.2898	0.1350	0.1343	0.1330	0.1347	0.1303
	down/min	−0.2849	−0.2845	−0.3069	−0.3069	−0.3112	−0.3834	−0.2738	−0.2705	−0.2835	−0.2821	−0.2792	−0.2829	−0.2735
	max	0.1357	0.1348	0.1775	0.1775	0.1783	0.2579	0.2903	0.2898	0.1350	0.1343	0.1330	0.1347	0.1303

an accurate description of the through-thickness transverse displacement variation u_ς is still of primary importance, so it is necessary to resort to higher-order theories.

Constraint stresses considerably modify the through-thickness distribution of $\sigma_{\alpha\varsigma}$ across the core and nearby the lower interface (Fig. 5), while they don't cause changes to the in-plane stresses. Again $\sigma_{\varsigma\varsigma}$ is no longer vanishing at the lower interface, where its magnitude is assumed to be $\sigma_{\varsigma\varsigma}^- = -5p_0^u$. Like for the previous thick case f, a large dispersion of results is shown by lower-order theories, therefore their inadequacy is confirmed.

4.4.3. Case h

The results for this case are reported in Table 8e. Again accurate results very close to FEA 3-D ones are obtained by adaptive theories ZZA, ZZA1, ZZA2, ZZA3, HWZZ and HWZZM, so it is confirmed that the choice of zig-zag is immaterial and that they can be also omitted if the procedure of (2.4) is used. In addition, it is confirmed that functions representing the variation of displacements across the thickness can be arbitrarily chosen under the same conditions. Lower order theories, in particular ones that incorporate standard Murakami's zig-zag function as layerwise function, appear still inadequate, at least with regards the prediction of u_ς, $\sigma_{\alpha\varsigma}$ and $\sigma_{\varsigma\varsigma}$.

Regarding the effect of constraint stresses, the application of $\sigma_{\varsigma\varsigma}^- = -5p_0^u$ at the supported edge induces a mutation of the trend of transverse shear and normal stresses across the core and across the upper face (Table 9d), which is incorrectly calculated by lower-order theories

Adaptive theories ZZA1, ZZA2, ZZA3, HWZZ and HWZZM once again prove to be the most accurate and efficient theories (see Table 6) for all cases f, g and h.

4.5. Case i – sandwich with stiff core and damaged lower face

In this case, a sandwich plate having the same geometric characteristics of case e but a much stiffer core and a damaged lower face [24] (E_{1111} E_{1122} E_{2222} E_{1212} are reduced by $2 \cdot 10^{-1}$ for Layer 1) is considered. Because of geometric and material asymmetries act jointly extolling each other, layerwise effects becomes stronger.

From Table 8f, which shows displacements and stresses predicted by all theories, an appreciable degree of accuracy emerges. However, theories based on Murakami's zig-zag function as the layerwise function turn out to be less accurate, because the slope of in-plane displacements reverses at the lower interface but not at the upper one like for case e. Because of this, lower-order theories MHR± and MHR4± obtain results similar to those of their counterparts MHR and MHR4, so not benefiting from the physical redefinition of the slope sign and also MHWZZA and MHWZZA4 are inaccurate despite having a higher-order kinematics.

The effect of the support reaction, namely the application of $\sigma_{\varsigma\varsigma}^- = -0.1p_0^u$ at the lower face takes place through a sharp rise of $\sigma_{\varsigma\varsigma}$ across the core, that doesn't change u_α and u_β whereas it changes considerably transverse shear stresses (Table 9e). The most evident effect of this is the increased disagreement among the predictions of lower and higher-order theories.

The accuracy and efficiency (see Table 6) of the adaptive theories are confirmed for this case, along with the possibility of arbitrarily choosing representation and zig-zag functions.

4.6. Case j – simply-supported sandwich plate with damaged thick core and face

A modified version of the three-layer, simply-supported sandwich plate under sinusoidal loading formerly considered by Zhen and Wanji [52] is now retaken assuming a damaged and thinner lower face (E_{1111} E_{1122} E_{2222} E_{1212} reduced by $1 \cdot 10^{-2}$) and a thicker core (that is partially damaged up to 0.15 h from below, E_{1122} E_{2222} E_{1212} E_{1313} E_{2323} are reduced by $2 \cdot 10^{-1}$). Due to such assumptions, this case extols the layerwise effects, similarly that in [24]. Transverse shear stresses reported in Table 8g show that the reduction of elastic moduli results into a totally different behavior from that of the undamaged case, while mild variations occurs for the other stresses and for displacements. Because, only an infinitesimal part of the bending stress is borne by the lower face, transverse shear stresses are strongly asymmetric across the thickness. Accordingly, the incorporation of layerwise functions able to accurately represent displacement and stress fields and the redefinition of coefficients across the thickness assume a primary importance. As the sign of $\sigma_{\beta\varsigma}$ reverses near

ARTICLE IN PRESS

Table 8e
Results for case h.

Case h		FEA 3-D	♠	HRZZ	HRZZ PP	HRZZ4	MHR MHR±	MHR4 MHR4±	MHWZZA	MHWZZA4	HWZZMC	HWZZMB2	HWZZMC2
		Theories											
u_α x10^{-4}	up	7.2089	7.2099	0.9979	0.9979	11.0672	6.9440	7.2027	21.2650	17.8713	6.5241	6.1033	6.5117
	down	−10.1752	−10.1700	−13.1971	−13.1971	−8.2691	−16.6906	−16.8561	−16.5921	−9.1610	−8.5017	−8.9046	−8.5017
	max	7.2089	7.2099	3.6072	3.6072	11.0672	6.9440	7.2027	23.7786	19.9744	6.5241	6.1033	6.5117
	min	−10.1752	−10.1700	−13.1971	−13.1971	−8.2691	−16.6906	−16.8561	−18.3875	−10.7021	−8.5017	−8.9046	−8.5017
u_ς x10^{-3}	up	1.6990	1.6952	0	1.3130	1.8381	0.8336	1.2080	1.4823	1.1463	1.6345	1.0837	1.6637
	max	1.6990	1.6952	0	1.3130	1.8381	0.8367	1.2100	1.4888	1.1551	1.6345	1.0837	1.6637
	min	0	0	0	−0.5875	−0.8226	0	0	0	0	0	0	0
$\sigma_{\alpha\alpha}$	up	0.0404	0.0402	0.4626	0.4626	−0.1183	0.1331	−0.2326	0.0679	−0.1504	−0.0680	−0.1063	−0.0712
	down/max	0.2127	0.2110	0.5066	0.5066	0.2864	−0.2018	0.2797	0.4976	0.3945	0.1005	0.1049	0.1017
	min	−0.1884	−0.1875	−0.5123	−0.5123	−0.2789	−0.3103	−0.2326	−0.5423	−0.4402	−0.0680	−0.1063	−0.0712
$\sigma_{\alpha\varsigma}$	max	0.1356	0.1357	2.7216	2.7216	0	0	0	0.3811	0.3988	0	0	0
	min	−5.1900	−5.1900	−7.6069	−7.6069	−5.7321	−2.5806	−2.5338	−8.5986	−8.5227	−4.4817	−4.0166	−4.6354
$\sigma_{\varsigma\varsigma}$	up	1.0000	1.0000	1.0000	1.0000	1.0000	1.0000	1.0000	1.0000	1.0000	1.0000	1.0000	1.0000
	max	1.0055	1.0055	1.1162	1.1162	''	''	''	1.0146	''	''	''	''

Table 8f
Results for case i.

Case i		FEA 3-D	♠	HRZZ	HRZZ PP	HRZZ4	MHR MHR±	MHR4 MHR4±	MHWZZA	MHWZZA4	HWZZMB	HWZZMC	HWZZMB2	HWZZMC2	HWZZM0
		Theories													
u_α x10^{-2}	up	−1.4225	−1.4259	−1.2851	−1.2851	−1.2737	−0.7871	−0.8028	−0.9253	−0.9346	−1.2903	−1.4250	−1.3000	−1.2911	−1.2991
	down/max	3.0175	3.0345	2.7807	2.7807	2.7522	1.0791	1.1007	2.2771	2.3001	2.4946	2.2230	2.4569	3.0535	2.4543
u_β x10^{-2}	up	−0.4742	−0.4741	−0.4284	−0.4284	−0.4246	−0.2714	−0.2768	−0.3117	−0.3086	−0.4328	−0.4749	−0.4334	−0.4280	−0.4316
	down/max	1.0059	1.0101	0.9269	0.9269	0.9174	0.3905	0.3983	0.7669	0.7592	0.8314	0.7443	0.8218	1.0257	0.8383
u_ς x10^{-2}	up	3.5705	3.5817	3.5238	3.3125	3.2903	2.4225	1.9379	2.1422	2.1850	3.2446	3.5889	2.4225	3.3502	3.2661
	down	3.9477	3.9430	3.5238	3.6207	3.5922	2.4515	2.7060	2.9220	2.9805	3.3662	3.3475	2.4515	3.9639	3.2389
$\sigma_{\alpha\alpha}$	up/max	65.5801	65.4700	59.2481	59.2481	58.7266	36.6356	37.3683	43.0362	42.6059	59.5049	65.6971	59.9352	59.5145	59.8889
	down	19.0188	19.0374	17.5260	17.5260	17.3462	10.9241	11.1426	14.4979	14.3529	15.7223	14.0245	15.4964	19.2775	15.5515
$\sigma_{\beta\beta}$	up	28.5252	28.5264	25.7727	25.7727	25.5460	16.2212	16.5457	18.6913	18.5044	25.9184	28.5742	26.0725	25.8587	26.0331
	down/max	38.6704	38.6763	35.6350	35.6350	35.2695	16.2723	16.5978	29.4769	29.1822	31.9686	28.4933	31.4897	39.1435	31.4861
$\sigma_{\alpha\beta}$	up/min	−13.8956	−13.9000	−12.5533	−12.5533	−12.4427	−7.8211	−7.9775	−9.1325	−9.2238	−12.6444	−13.9184	−12.7001	−12.5776	−12.6695
	down	7.3693	7.3791	6.7909	6.7909	6.7212	2.1139	2.1562	5.6179	5.6741	6.0917	5.4411	6.0103	7.4860	6.0677
$\sigma_{\alpha\varsigma}$	max	22.5907	22.4046	19.7134	19.7134	19.4974	20.3905	22.4648	21.9681	21.9681	20.3015	22.3695	20.4425	19.6569	20.4280
	min	−10.4100	−10.1051	−9.3251	−9.3251	−9.2209	−0.3555	−5.1433	−10.2517	−10.2497	−8.4004	−6.9932	−8.1893	−10.2830	−8.1850
$\sigma_{\beta\varsigma}$	max	7.4682	7.4796	6.5711	6.5711	6.4991	6.5250	6.4090	5.3118	5.3649	6.7948	7.4550	6.8151	6.5281	6.7946
	min	−3.3684	−3.3567	−3.1084	−3.1084	−3.0736	−0.1138	−1.4673	−2.6080	−2.6341	−2.8006	−2.3197	−2.7203	−3.4008	−2.6599
$\sigma_{\varsigma\varsigma}$	min	−1.1414	−1.1359	−1.0101	−1.0101	−0.9963	−0.0069	−0.3866	−1.5002	−1.4852	−0.9947	−0.6882	−0.8281	−1.4545	−0.9251

Table 8g
Results for case j.

Case j		FEA 3-D	♠	HRZZ	HRZZ PP	HRZZ4	MHR	MHR4	MHR±	MHR4±	MHWZZA	MHWZZA4	HWZZMB	HWZZMC	HWZZMB2	HWZZMC2
u_α	up/min	−0.3828	−0.3866	−0.3848	−0.3848	−0.3689	−0.3702	−0.3753	−0.3296	−0.3304	−0.3834	−0.3828	−0.3874	−0.4122	−0.4199	−0.3702
x10^{-2}	down/max	4.6261	4.6723	4.8664	4.8664	4.5824	4.7763	4.9984	4.1652	3.9997	4.6581	4.6412	3.7539	4.9763	4.1339	4.7763
u_β	up/min	−0.0443	−0.0444	−0.0441	−0.0441	−0.0430	−0.0546	−0.0541	−0.0518	−0.0508	−0.0429	−0.0439	−0.0559	−0.0471	−0.0431	−0.0473
x10^{-1}	down/max	1.0694	1.0712	1.0981	1.0981	1.0499	0.7801	0.7865	0.7420	0.7045	1.0772	1.0726	0.8773	1.1537	1.1015	1.1580
u_ς	up	0.9619	0.9613	0.9683	0.9655	0.9677	0.0927	0.0930	0.9431	0.9556	0.9649	0.9618	0.9731	1.0388	0.8940	1.0451
x10^{-1}	down/min	0.8307	0.8306	0.9683	0.8312	0.8113	0.7956	0.7649	0.8103	0.7508	0.8332	0.8308	0.9287	0.8964	0.8427	0.9042
$\sigma_{\alpha\alpha}$	up/max	32.8699	32.8733	33.0394	33.0394	31.6808	31.9053	32.3405	35.4284	35.5056	32.9073	32.8665	33.3650	35.3858	23.5493	35.5898
	down	0.6546	0.6512	0.6156	0.6156	0.6234	−0.2182	−0.3109	−0.5368	−0.5376	0.6628	0.6585	0.5587	0.7144	1.6309	0.7188
$\sigma_{\beta\beta}$	up	1.8425	1.8367	1.8369	1.8369	1.7880	2.1963	2.1852	2.1387	2.1065	1.7960	1.8299	2.2457	1.9630	1.7309	1.9713
	down/max	3.3715	3.3631	3.4948	3.4948	3.3219	2.8462	2.9200	2.8904	2.7598	3.3974	3.3838	2.7553	3.6340	2.9191	3.6468
$\sigma_{\alpha\beta}$	up/min	−1.3986	−1.4076	−1.3983	−1.3983	−1.3537	−1.5513	−1.5524	−1.5757	−1.5609	−1.3761	−1.3923	−1.6018	−1.4960	−1.2043	−1.5032
	down	0.2595	0.2573	0.2684	0.2684	0.2555	0.2130	0.2178	0.2138	0.2040	0.2179	0.2180	0.2122	0.2797	0.2333	0.2807
$\sigma_{\alpha\varsigma}$	max	11.1897	11.1938	10.8151	10.8151	10.9233	10.1734	9.7946	10.2751	10.0958	10.6435	11.1353	11.8110	12.1571	11.2785	12.2440
	min	−0.2687	−0.2697	−0.4964	−0.4964	−0.5014	0	0	0	0	−0.1740	−0.9738	−0.0951	−0.2832	−0.2744	−0.2784
$\sigma_{\beta\varsigma}$	max	1.1471	1.1381	1.1243	1.1243	0.9280	1.6464	1.5236	1.5425	1.3516	1.1096	1.1430	2.1697	2.0520	1.3254	1.2852
	min	−1.9038	−1.9038	−1.9937	−1.9937	−1.9431	−1.6117	−1.6532	−1.6381	−1.5689	−1.9259	−1.9181	−1.6823	−1.2632	−1.2818	−2.0547
$\sigma_{\varsigma\varsigma}$	min	−0.3524	−0.3530	−0.3253	−0.3253	−0.2348	−0.0860	−0.0795	−0.0666	−0.0630	−0.3509	−0.3501	−0.0008	−0.0105	−0.0067	−0.0101

Above the first row of data, spanning the theory columns: **Theories**

Table 8h
Results for case k.

Case k		FEA 3-D	♠	HRZZ	HRZZ PP	HRZZ4	MHR MHR±	MHR4 MHR4±	MHWZZA	MHWZZA4	HWZZMB	HWZZMC	HWZZMB2	HWZZMC2	HWZZM0
u_α, u_β	up/min	−2.2761	−2.2728	−2.3900	−2.3900	−2.4562	−2.4379	−2.4282	−0.7415	−0.7341	−2.5117	−2.1903	−2.3112	−2.2700	−2.3556
x10^{-3}	down/max	2.6229	2.6189	2.7929	2.7929	2.7623	2.2598	2.2417	3.2909	3.2580	2.7904	3.2180	2.9162	3.0627	1.9739
	up	3.9097	3.9083	3.4482	3.8811	3.8802	3.4655	1.3704	2.9731	3.0326	3.5052	3.7750	3.8088	3.7484	3.2561
u_ς	down/min	3.5811	3.5819	3.4482	3.5326	3.5338	3.4489	0.9300	2.5671	2.6184	3.4224	3.1317	3.7892	3.2986	3.2552
x10^{-2}	max	3.9142	3.9120	3.4482	3.8864	3.8857	3.4748	1.3778	2.9737	3.0332	3.5112	3.7813	3.8148	3.7546	3.2619
$\sigma_{\alpha\alpha}$, $\sigma_{\beta\beta}$	up/max	1.3294	1.3326	1.2748	1.2748	1.3090	1.2996	1.5583	1.4536	1.4623	1.4360	1.3914	1.3936	1.4064	1.3752
	down/min	−1.5510	−1.5605	−1.4437	−1.4437	−1.4279	−1.1681	−1.1422	−1.6959	−1.7061	−1.4921	−1.5756	−1.5232	−1.5623	−1.0658
$\sigma_{\alpha\beta}$	up/min	−0.2805	−0.2808	−0.3111	−0.3111	−0.3198	−0.3174	−0.3567	−0.3647	−0.3683	−0.3422	−0.3631	−0.3482	−0.3598	−0.3334
	down/max	0.3168	0.3168	0.3636	0.3636	0.3596	0.2942	0.2859	0.4119	0.4160	0.3525	0.3363	0.3509	0.3504	0.2543

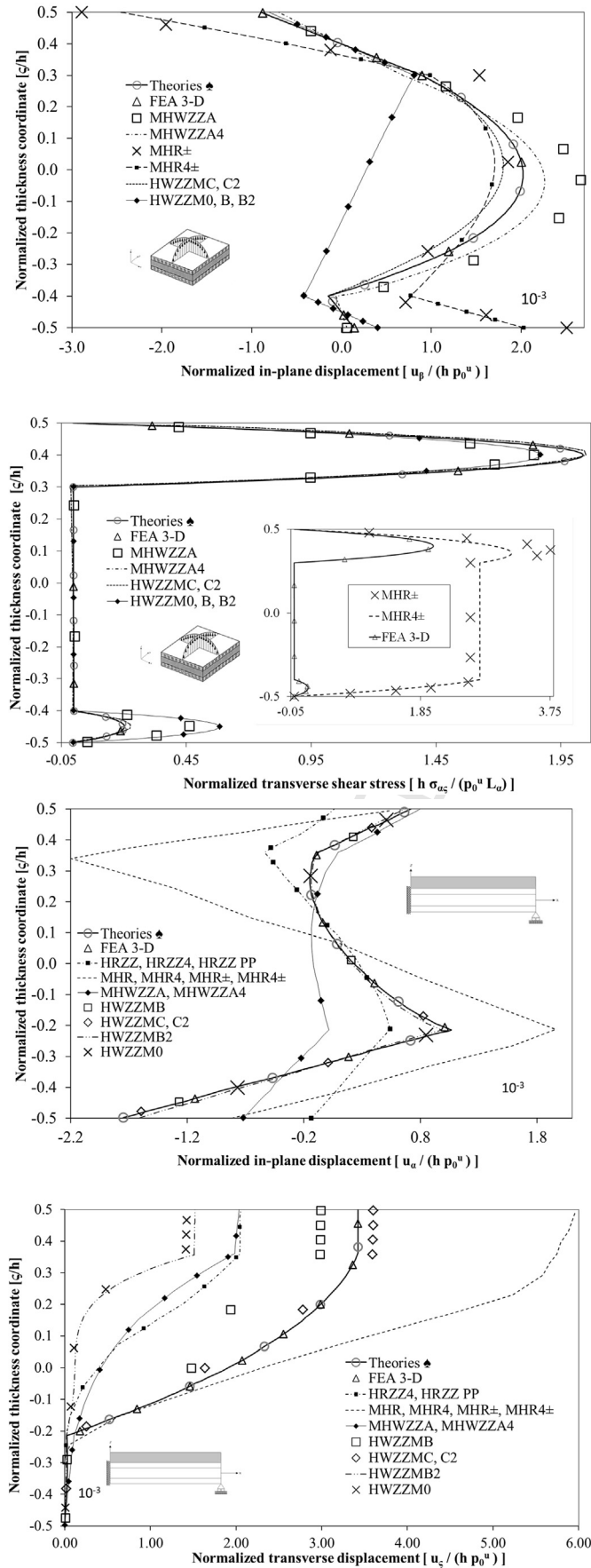Above the first row of data, spanning the theory columns: **Theories**

Fig. 1. Case e: Simply supported rectangular sandwich plate ($L_\alpha/h = 4$, $L_\beta/L_\alpha = 3$) under a bisinusoidal loading applied on the top layer considering the effects of support reactions.

Table 9a

Results for case d – with support reaction; ♠ ZZA, ZZA1, ZZA2, ZZA3, HWZZ, HWZZM, coincident results.

Case d		FEA 3-D	♠	MHWZZA	MHWZZA4	MHR±	MHR4±	HWZZMB	HWZZMC	HWZZMB2	HWZZMC2	HWZZM0
				Theories								
u_α	up/min	−3.0069	−2.9857	−3.1698	−3.8699	−2.8732	−3.0673	−3.2186	−3.2972	−2.8802	−3.1961	−2.9075
	down/max	1.3868	1.3977	1.2477	1.3531	1.1323	1.2296	1.4686	1.4759	1.2182	1.4493	1.3226
$\sigma_{\alpha\varsigma}$	max	2.0596	2.0571	2.1065	2.1584	2.0978	2.0943	2.2695	2.2919	1.9520	2.2717	2.0733

Table 9b

Results for case e – with support reaction.

Case e		FEA 3-D	♠	MHWZZA	MHWZZA4	MHR±	MHR4±	HWZZMB	HWZZMC	HWZZMB2	HWZZMC2	HWZZM0
				Theories								
u_α	up/min	−3.6000	−3.6099	0.8988	−3.2460	−8.5408	−7.2316	−3.9382	−4.0447	−3.8085	−4.2308	−3.7886
$\times 10^{-5}$	down	0.5789	0.5731	−0.0387	−0.0121	7.3054	5.8687	1.8905	0.6141	1.9420	0.6959	1.9459
	max	8.1439	8.1465	6.2363	8.0957	7.3054	5.8687	3.8395	8.3408	3.8842	8.6421	3.8969
$\sigma_{\beta\varsigma}$	max	2.7161	2.7167	2.5739	2.5739	1.8468	1.5700	2.3857	2.7134	2.4645	2.7135	2.4900

Table 9c

Results for case f – with support reaction.

Case f		FEA 3-D	♠	HWZZ	MHWZZA	MHWZZA4	MHR±	MHR4±	HWZZMB	HWZZMC	HWZZMB2	HWZZMC2	HWZZM0
					Theories								
u_α	up	0.7593	0.7523	0.7524	3.4949	3.5648	0.5081	0.4110	0.7060	0.7478	0.6185	0.7446	0.6597
$\times 10^{-3}$	down	−1.8370	−1.8346	−1.8348	−2.3827	−2.4304	−0.7616	−0.6161	−1.7215	−1.8234	−1.5082	−1.8158	−1.6086
	max	1.1156	1.1156	1.1157	3.4949	3.5648	1.8274	1.4781	1.0469	1.1088	0.9171	1.1042	0.9782
	min	−1.8370	−1.8346	−1.8348	−2.3827	−2.4304	−2.0502	−1.6584	−1.7215	−1.8234	−1.5082	−1.8158	−1.6086

Table 9d

Results for case h – with support reaction.

Case h		FEA 3-D	♠	MHWZZA	MHWZZA4	MHR±	MHR4±	HWZZMC	HWZZMB2	HWZZMC2
				Theories						
u_α	up	7.8480	7.8480	21.7754	17.1564	7.1315	7.3036	6.4327	6.0362	6.3880
$\times 10^{-4}$	down	−10.7238	−10.7431	−16.9903	−8.7945	−17.1413	−17.0921	−8.3827	−8.8067	−8.3402
	max	7.8480	7.8480	24.3493	19.1754	7.1315	7.3036	6.4327	6.0362	6.3880
	min	−10.7238	−10.7431	−18.8288	−10.2740	−17.1413	−17.0921	−8.3827	−8.8067	−8.3402
$\sigma_{\alpha\varsigma}$	max	0.2881	0.2882	1.3648	0.3313	0	0	0	0	0
	min	−5.1540	−5.1702	−8.8055	−8.2333	−2.6503	−2.5705	−4.4190	−3.9742	−4.5496
$\sigma_{\varsigma\varsigma}$	max	1.0580	1.0581	1.3576	1.0000	1.0000	1.0000	1.0000	1.0000	1.0000

Table 9e

Results for case i – with support reaction.

| Case i		FEA 3-D	♠	MHWZZA	MHWZZA4	MHR±	MHR4±	HWZZMB	HWZZMC	HWZZMB2	HWZZMC2	HWZZM0
				Theories								
u_α	up	−1.1759	−1.1757	−1.2443	−1.2634	−2.1116	−2.4988	−1.3408	−1.4566	−1.3479	−1.3328	−1.3545
$\times 10^{-2}$	down/min	3.5337	3.5304	2.7249	2.6477	1.7136	−2.0539	2.5877	2.1695	2.4441	3.0547	2.4648
	min	−3.7376	−3.7374	−2.9052	−2.9369	−2.1116	−9.6905	−2.6303	−3.0659	−2.7200	−3.3067	−2.7414
u_β	up	−0.3897	−0.3898	−0.4977	−0.5054	−0.7176	−0.8014	−0.4473	−0.4859	−0.4497	−0.4437	−0.4519
$\times 10^{-2}$	down/max	1.1795	1.1775	1.0900	1.0591	0.5931	−0.7475	0.8621	0.7135	0.8129	1.0169	0.8197
	min	−1.2444	−1.2449	−1.1621	−1.1748	−0.7176	−3.2920	−0.8773	−1.0316	−0.9085	−1.1036	−0.9157
$\sigma_{\alpha\varsigma}$	max	16.3209	16.3762	22.7094	21.7916	9.3027	8.8559	20.6429	22.3609	20.7514	19.8125	20.8607
	min	−11.8300	−11.6960	−9.9516	−10.3215	0.0000	0.0000	−8.4423	−6.5053	−8.2366	−10.4128	−8.2800
$\sigma_{\beta\varsigma}$	max	5.4438	5.4406	8.1223	8.4631	3.1401	2.8886	6.8883	7.4608	6.6014	6.9245	6.9610
	min	−3.8950	−3.8984	−3.6242	−3.4967	0.0000	0.0000	−2.8171	−2.2016	−3.4771	−2.7531	−2.7675
$\sigma_{\varsigma\varsigma}$	min	−0.3639	−0.3692	−0.2210	−0.2210	−0.1000	−0.1000	−0.1954	−0.1527	−0.1896	−0.2426	−0.1894

the lower face and that of $\sigma_{\zeta\zeta}$ exhibits a through-thickness change, capturing these stress fields is rather challenging. For this reason, strong discrepancies appear between the predictions of the lower-order theories. Because Murakami's rule of a reversing slope at material interfaces fails, theories using Murakami's zig-zag functions fail to be accurate. In this case, quite accurate results for $\sigma_{\alpha\varsigma}$ are provided by HWZZMB, HWZZMB2, HWZZMC, HWZZMC2, while HWZZMA and HWZZM0 cannot be equally effective. Also in this case it is confirmed that zig-zag functions can be arbitrarily chosen or even omitted and that also the representation can be arbitrarily chosen without any loss of accuracy.

Table 9f
Results for case j – with support reaction.

Case j		FEA 3-D	♠	MHWZZA	MHWZZA4	MHR±	MHR4±	HWZZMB	HWZZMC	HWZZMB2	HWZZMC2
u_α	up/min	−0.3914	−0.3914	−0.5230	−0.3477	−0.3325	−0.3298	−0.2653	−0.3295	−0.3065	−0.3295
x10^{-2}	down/max	4.9514	4.9513	4.2420	4.6688	4.5997	4.6120	2.5716	3.7772	2.9749	3.7915
u_β	up/min	−0.0451	−0.0451	0.0970	−0.0078	−0.0416	−0.0419	−0.0416	−0.0384	−0.0233	−0.0416
x10^{-1}	down/max	1.1409	1.1428	0.9030	1.0922	0.6770	0.6885	0.8688	0.6018	0.5878	0.8723
$\sigma_{\alpha\varsigma}$	max	10.5784	10.5715	10.7787	10.7787	9.8716	9.7930	7.9505	9.8004	7.5349	9.7887
	min	−0.3540	−0.3545	0	0	0	0	−0.0534	−0.0838	−0.1594	−0.0822
$\sigma_{\beta\varsigma}$	max	1.3089	1.3078	1.5140	1.5140	1.1413	1.1375	−0.8593	−1.4083	0.6000	1.3672
	min	−2.1055	−2.1066	−2.0737	−2.0737	−1.4485	−1.4626	1.0911	1.3756	−1.1206	−1.4205
$\sigma_{\varsigma\varsigma}$	min	−0.1389	−0.1383	−0.1141	−0.1087	−0.1079	−0.1080	−0.1019	−0.1046	−0.1000	−0.1047

Table 9g
Results for case k – with support reaction.

Case k		FEA 3-D	♠	MHWZZA	MHWZZA4	MHR±	MHR4±	HWZZMB	HWZZMC	HWZZMB2	HWZZMC2	HWZZM0
u_α, u_β	up/min	−2.5495	−2.5435	−0.5455	−0.8797	−3.1143	−0.3533	−2.3844	−2.4250	−2.6578	−2.2822	−2.6864
x10^{-3}	down/max	2.8374	2.8381	3.3057	3.4821	3.1896	3.1504	2.9450	2.7453	2.6614	2.6944	2.6725
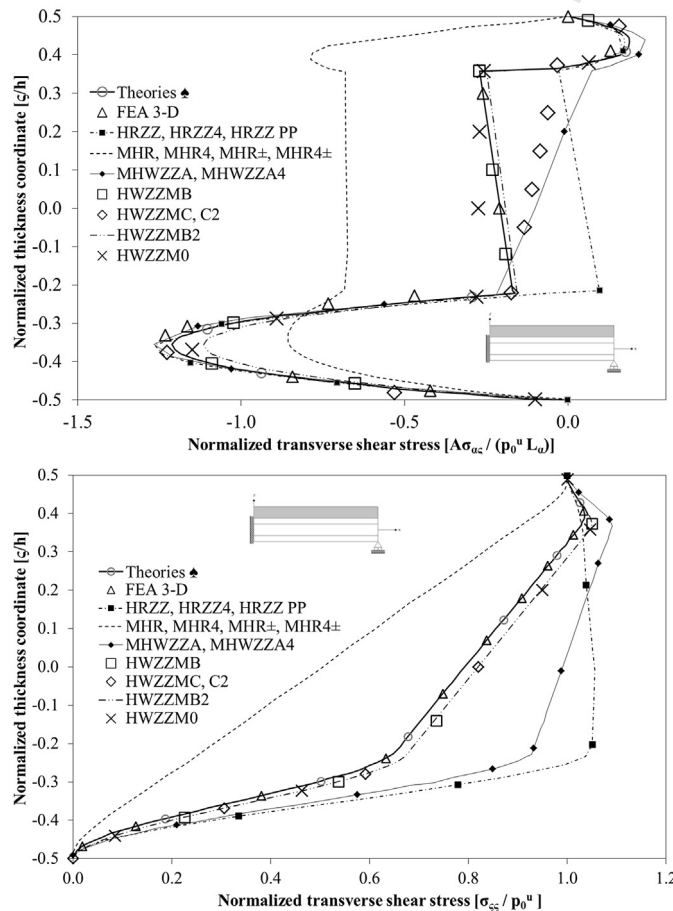
Fig. 2. Case f: Propped-cantilever sandwich beam ($L_\alpha/h = 5.714$) under a uniform loading on the top layer.

Unlike for the previous cases, the effect of constraint stresses ($\sigma_{\varsigma\varsigma}^- = -0.1 p_0^u$) does not change significantly the through-thickness distribution of transverse shear stresses and in-plane displacements (Table 9f). Also in this case adaptive theories ZZA1, ZZA2, ZZA3, HWZZ and HWZZM appear as the most efficient theories as shown by Table 6, since they have a high accuracy and low computational costs.
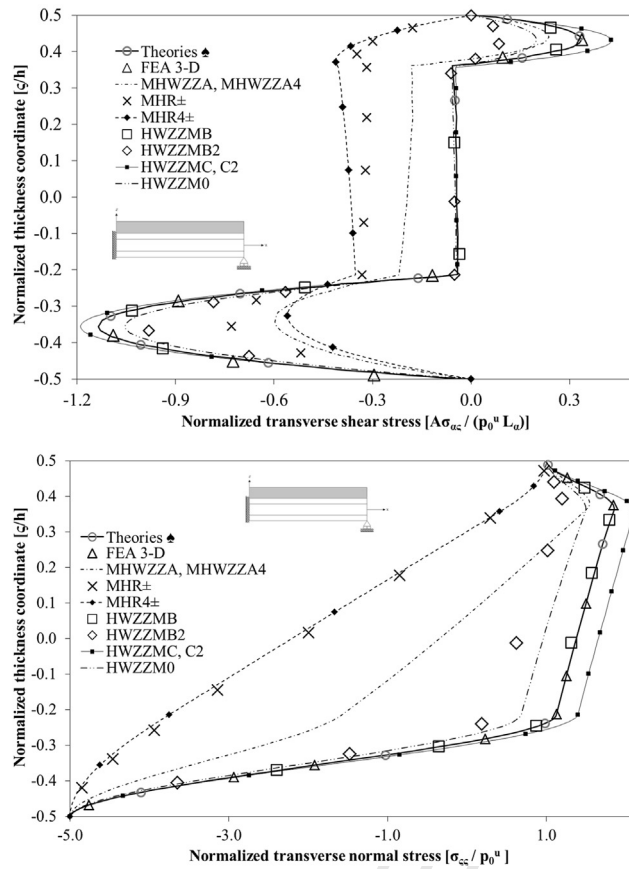
Fig. 3. Case f: Propped-cantilever sandwich beam ($L_\alpha/h = 5.714$) under a uniform loading on the top layer considering the effects of support reactions.
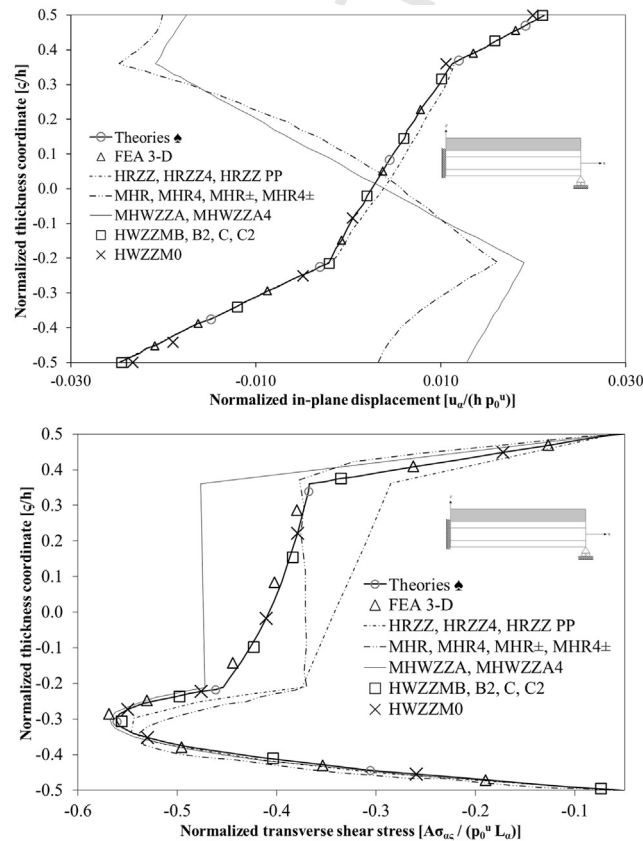
Fig. 4. Case g: Propped-cantilever sandwich beam ($L_\alpha/h = 20$) under a uniform loading on the top layer.
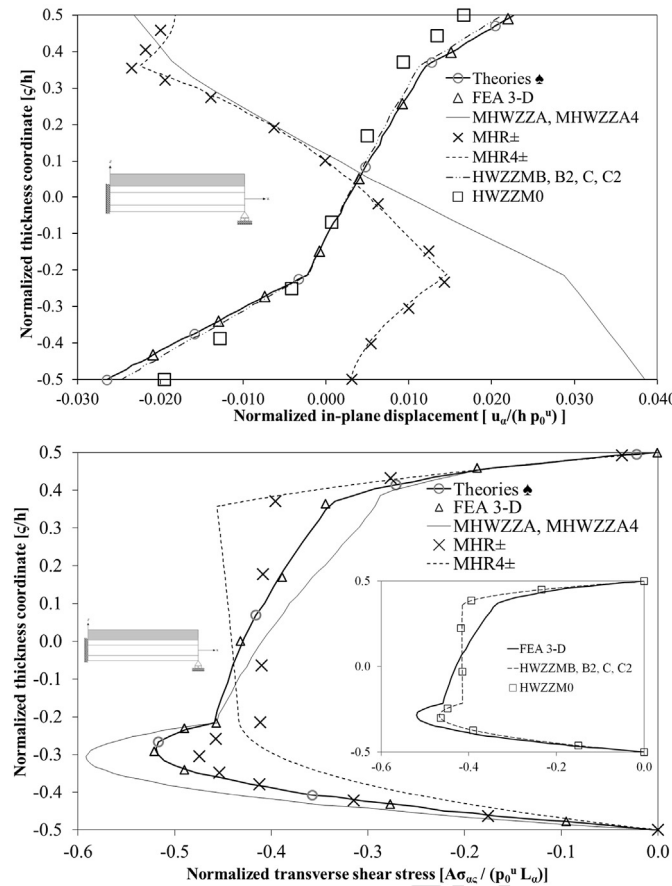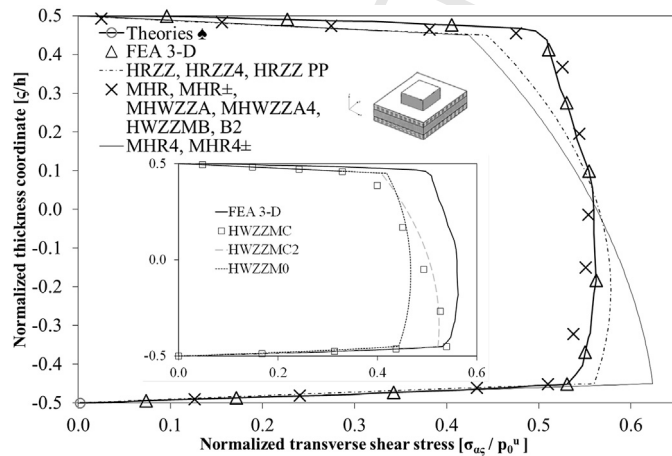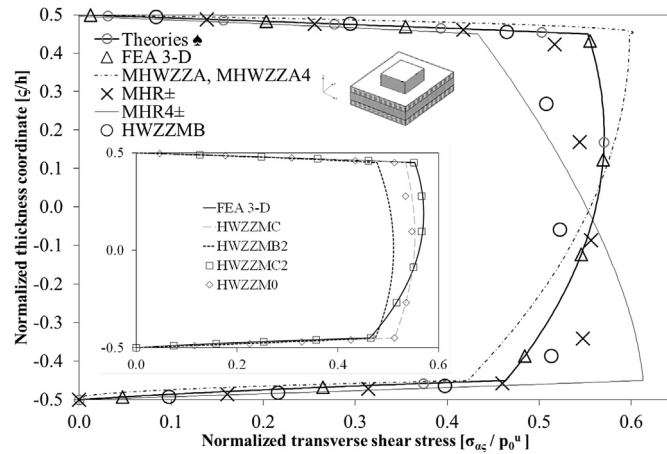
Fig. 5. Case g: Propped-cantilever sandwich beam ($L_\alpha/h = 20$) under a uniform loading on the top layer considering the effects of support reactions.

Fig. 6. Case k: Simply supported square sandwich plate ($L_\alpha/h = 4$) subjected to a local uniform loading on the top layer applied in $L_\alpha/4 \leq \alpha \leq 3L_\alpha/4$, $L_\beta/4 \leq \beta \leq 3L_\beta/4$.

4.7. Case k – sandwich plate with thin faces

As last case, a simply-supported sandwich plate with thin faces is considered, which is undergoing a uniform locally applied load at the center of its upper face (load from $\alpha = L_\alpha/4$ to $\alpha = 3L_\alpha/4$ and from $\beta = L_\beta/4$ to $\beta = 3L_\beta/4$) [24]. All constituent materials are assumed to be isotropic. Fig. 6 and Table 8h show the through-thickness distribution of displacements and stresses for this case. Structure and loading being symmetric, it occurs that $\sigma_{\alpha\xi} = \sigma_{\beta\varsigma}$, $\sigma_{\alpha\alpha} = \sigma_{\beta\beta}$, $u_\alpha = u_\beta$ on the respective sides. For this case, results by MHR, MHR±, MHWZZA, MHWZZA4, HWZZMB and HWZZMB2 are merged together in Fig. 6, for sake of brevity, because their findings are very similar. Adaptive theories ZZA, ZZA1, ZZA2, ZZA3, HWZZ and HWZZM as well as theories HWZZMB and HWZZMB2 prove to accurately predict all through-thickness stress and displacement fields.

Although a better agreement among the predictions of lower order theories is shown than in the previous cases, lower order theories still appear rather inaccurate. MHR4 misestimates the magnitude of displacements and stresses, due to the incorrect representation of the slope sign variation at interfaces. However, accuracy does not increase for MHR4±, as a consequence of their still too poor kinematics. Instead, transverse shear stress is quite accurately predicted by MHR and MHR±. HWZZMA is inaccurate because the recalculation of

Fig. 7. Case k: Simply supported square sandwich plate ($L_\alpha/h = 4$) subjected to a local uniform loading on the top layer applied in $L_\alpha/4 \le \alpha \le 3L_\alpha/4$, $L_\beta/4 \le \beta \le 3L_\beta/4$ considering the effects of support reactions.

zig-zag amplitudes at each interface is omitted. From this fact and given the high accuracy of adaptive theories is proven again that the choice of zig-zag functions is immaterial and moreover that any function can be used in order to express transverse displacements without any loss of accuracy only for adaptive theories.

Here again the support reaction ($\sigma_{\varsigma\varsigma}^- = -0.02 p_0^u$) leaves unchanged displacements and in-plane stresses, while it considerably changes the transverse shear stresses across the thickness (Fig. 7 and Table 9g). In this case, HWZZMC2, MHWZZA and MHWZZA4 give results that are in very good agreement with HWZZ, ZZA, ZZA1, ZZA2, ZZA3, HWZZ. On the contrary HWZZMB, HWZZMB2, HWZZMC and HWZZM0 provide inaccurate results. Results by HRZZ, HRZZPP, HRZZA4, MHR and MHR4 are again to poor, so they are not reported in Fig. 7.

Adaptive theories ZZA1, ZZA2, ZZA3, HWZZ and HWZZM prove to be the most efficient ones also for this case (see Table 6).

5. Concluding remarks

Accuracy of various theories, some of which are new while others are retaken from previous papers by the authors, have been assessed. They derive from the ZZA 3-D zig-zag theory [26] under steadily growing limiting assumptions on displacement, strain and stress fields. As they differ by the choice of through-thickness functions representing variables and of zig-zag layerwise functions, the aim of the present study is to demonstrate numerically that the choice of such functions can be immaterial whenever their coefficients are recomputed across the thickness by enforcing the same whole set of constraint conditions (e.g., stress compatibility at interfaces, stress boundary conditions and fulfillment of local equilibrium equations), provided that their expressions are obtained in exact form via symbolic calculus.

As the symbolic calculus tool used finds once and for all closed-form expressions of coefficients, it constitutes an automatic support that enables users to choose the coarse representation and the zig-zag functions as desired. Its use enables a variable-kinematic representation while keeping fixed the number of functional d.o.f., here assumed coinciding with the classical five middle-plane displacements and rotations of the normal (but any other combination could be used).

Challenging benchmarks with strong layerwise effects, where an accurate description of the normal transverse deformation is required, are considered for testing theories. They present a quite large variation of mechanical properties of constituent layers, a low length-to-thickness ratio (but results for rather slender cases are also presented), different lay-ups, loadings and simply-supported or clamped edges (in the first case also the effects of support stresses are considered).

Closed form solutions to elastostatic problems considered are obtained using the same trial functions and the same type and order of expansion of the in-plane representation for all theories, to compare them under the same conditions. As regards the representation across the thickness, the expansion order is limited to the third-order for the in-plane displacements and to the fourth-order for the transverse one. This because the redefinition of coefficients makes superfluous use of higher orders, fact that makes the present theories very efficient.

The numerical results prove the thesis of this paper and precisely that that if all the physically admissible constraint conditions are enforced, theories with different zig-zag functions lead to the same results.

The same holds as regards the choice of the representation functions. So the choice of the functions used to represent variables across the thickness and of zig-zag functions can be arbitrary assumed without the results showing inaccuracies. Zig-zag functions can even be omitted when a number of unknown coefficients equal to the number of zig-zag amplitudes is incorporated, whose expressions are determined by enforcing the fulfillment of interfacial stress compatibility conditions.

Vice-versa, the accuracy of the theories that impose only a partial set of physical constraints are largely dependent upon the choice of the aforementioned parameters, the accuracy of results being highly susceptible to the variation of layer thickness and elastic properties assumed.

Theories based on Murakami's like zig-zag function as the layerwise function appear less accurate than physically-based counterparts with the same order of expansion across the thickness, as in many of the cases considered the slope of displacements doesn't always reverse at interfaces.

Numerical results show unequivocally that more accurate predictions of through-thickness displacement and stress fields are achieved by the theories incorporating a piecewise zig-zag variation of the transverse displacement. Physically-based theories of this paper get through-thickness displacement and stress fields as accurately as theories by other researchers, which assume an order of expansion of

the variables across the thickness much higher. A simplified uniform or polynomial representation of the transverse displacement is shown ineffective even when strain and stress fields retaken from more accurate models are incorporated into mixed theories.

The previous considerations remain valid even when slender cases are considered, because although transverse normal deformability effects are no longer dominant, the shortcomings of lower-order theories are magnified by the increased magnitude of deflection.

The support reaction $\sigma_{\varsigma\varsigma}$ could change considerably the through-thickness filed of transverse shear stresses even when having a small magnitude, while it leaves virtually unchanged in-plane stresses and displacements.

Declaration of competing interest

The authors declare that they have no known competing financial interests or personal relationships that could have appeared to influence the work reported in this paper.

Appendix A. Symbolic calculus tool

Here, the steps for constructing the structural model is discussed. Note that the procedure is valid irrespective of the theory because the only thing that sets apart theories is the formulation of the displacement field starting from which the calculation proceeds automatically according to the instructions given below. The process is completely automatic and allows the user to choose the functions of representation and zigzag functions, as well as loadings at will, always obtaining an exact formulation of the model coefficients. In this framework, every sort of theory can be developed including those with only partial satisfaction of constraints. This allows users to compare many theories and understand which ones are advantageous. Program is developed under MathWorks-CAMPUS WIDE (Politecnico di Torino).

```
%% CREATION OF SYMBOLIC VARIABLES (example refers to a beam)
    for i = 1:M %M is the number of terms of in-plane expansion
        vettAmn(i) = sym(strcat('Amn_',num2str( i )),'real');
        vettCmn(i) = sym(strcat('Cmn_',num2str(i)),'real');
        vettDmn(i) = sym(strcat('Dmn_',num2str(i)),'real');
    end
dofRR=[vettAmn,vettCmn,vettDmn]';
%example for a beam
p0u = sym('p0u','real');    %symbolic loading p_0^u
z = sym('z', 'real');    %transverse coordinate ς
x = sym('x','real');    %in-plane coordinate α
...
...   %(This apply for all variables)
...
    end
       end
          end
         %   u = u_α    w = u_ς
%%% USER
```

This is the only things that user must specify, which is the only thing that characterizes theories

```
% Next steps are carried out automatically

%% CONSTRUCTION OF STRAIN AND STRESS FIELDS
%diff: Differentiate symbolic expression or function respect the indicate variable
epsx = diff(u,x);   % epsx  = ε_αα
...
epsz = diff(w,z);   % epsz = ε_ςς
...
epsxz= diff(u,z)+diff(w,x);   % epsxz = ε_ας
for i = 1:nl
    mia_Q = Q(:,:,i);
    epsilon = [epsx(i)...]';
    sigmax(i) = (mia_Q(1,:)* epsilon)';   % sigmax = σ_αα     sigmaxz = σ_ας  sigmaz = σ_ςς
    ...
end

%% ENFORCEMENT OF PHYSICAL CONSTRAINTS
%e.g. sigmaxz = 0 at upper and lower layers
%posxz_x: definition of in-plane position where constraint is imposed (numerical variable)
cont = 1; %counter
sigmaxzL = sigmaxz(1);
F(cont,1) = sigmaxzL;   %equivalent to imposition of sigmaxzL = 0;
```

F(cont,1) = subs(F(cont,1),x,posxz_x);

F(cont,1) = subs(F(cont,1),z,−0.5 *h);*

cont = cont+1;

sigmaxzU = sigmaxz(nl);

F(cont,1) = F(cont,1)+sigmaxzU;

F(cont,1) = subs(F(cont,1),x,posxz_x);

F(cont,1) = subs(F(cont,1),z ,+0.5 *h);*

cont = cont + 1;

%Repeat for other constraints

%F will contain all the boundary, compatibility and equilibrium equations

%% CALCULATION OF COEFFICIENTS BY CONSTRAINTS

%Cost_sist contains the coefficients that are calculated by imposing the fulfillment of conditions F

%The number and which coefficients are contained in Cost_sist is chosen by user.

%Number of equations of F must be the same of Cost_sist

F = subs(vpa(F),p0u,p0u_num); %p0u_num is the numerical value of load

solut = vpasolve(F,Cost_sist);

Actually the displacement field is completely defined, by substituting back expressions *solut*.

Procedure continues building the functional. The example refers to Total potential energy functional.

%% SOLUTION BY RR METHOD

%TOT_POT: total potential energy

%Symbolic integration may be carried out by int function, but a

%numerical approach is equally accurate and requires a lower effort.

%dofRR contains the remaining unknown amplitudes that are not yet

%determined by solving the previous system of equations F.

   cont = 1;

   for i = 1:length(dofRR)

     F2(cont,1) = diff({TOT_POT},dofRR(i));

     cont = cont + 1;

   end

F2 = subs(vpa(F2),p0u,p0u_num);

soluz = vpasolve(F2,dofRR);

The problem is solved and the results can be plotted.

References

[1] J.N. Reddy, Mechanics of Laminated Composite Plates and Shells: Theory and Analysis, 2nd edition, CRC Press, Boca Raton, 2003.

[2] V.V. Vasilive, S.A. Lur'e, On refined theories of beams, plates and shells, J. Compos. Mater. 26 (1992) 422–430.

[3] J.N. Reddy, D.H. Robbins, Theories and computational models for composite laminates, Appl. Mech. Rev. 47 (1994) 147–165.

[4] S.A. Lur'e, N.P. Shumova, Kinematic models of refined theories concerning composite beams plates and shells, Int. Appl. Mech. 32 (1996) 422–430.

[5] A.K. Noor, S.W. Burton, C.W. Bert, Computational model for sandwich panels and shells, Appl. Mech. Rev. 49 (1996) 155–199.

[6] H. Altenbach, Theories for laminated and sandwich plates. A review, Int. Appl. Mech. 34 (1998) 243–252.

[7] E. Carrera, Developments, ideas, and evaluations based upon Reissner's mixed variational theorem in the modeling of multilayered plates and shells, Appl. Mech. Rev. 54 (2001) 301–329.

[8] E. Carrera, Historical review of zig-zag theories for multilayered plates and shells, Appl. Mech. Rev. 56 (2003) 1–22.

[9] E. Carrera, On the use of the Murakami's zig-zag function in the modeling of layered plates and shells, Compos. Struct. 82 (2004) 541–554.

[10] L. Demasi, Refined multilayered plate elements based on Murakami zig-zag functions, Compos. Struct. 70 (2004) 308–316.

[11] L. Demasi, Mixed plate theories based on the generalized unified formulation. Part IV: zig-zag theories, Compos. Struct. 87 (2009) 195–205.

[12] R. Khandan, S. Noroozi, P. Sewell, J. Vinney, The development of laminated composite plate theories: a review, J. Mater. Sci. 47 (2012) 5901–5910.

[13] S. Kapuria, J.K. Nath, On the accuracy of recent global–local theories for bending and vibration of laminated plates, Compos. Struct. 95 (2013) 163–172.

[14] M. Di Sciuva, A refinement of the transverse shear deformation theory for multilayered orthotropic plates, L'Aerotecnica Missili e Spazio 62 (1984) 84–92.

[15] H. Murakami, Laminated composite plate theory with improved in-plane responses, J. Appl. Mech. 53 (1986) 661–666.

[16] E. Carrera, An assessment of mixed and classical theories on global and local response of multilayered orthotropic plates, Compos. Struct. 50 (2000) 183–198.

[17] E. Carrera, M. Filippi, E. Zappino, Laminated beam analysis by polynomial, trigonometric, exponential and zig-zag theories, Eur. J. Mech. A, Solids 41 (2013) 58–69.

[18] J.D. Rodrigues, C.M.C. Roque, A.J.M. Ferreira, E. Carrera, M. Cinefra, Radial basis functions-finite differences collocation and a unified formulation for bending, vibration and buckling analysis of laminated plates, according to Murakami's zig-zag theory, Compos. Struct. 93 (2011) 1613–1620.

[19] U. Icardi, Higher-order zig-zag model for analysis of thick composite beams with inclusion of transverse normal stress and sublaminates approximations, Composites, Part B, Eng. 32 (2001) 343–354.

[20] X.Y. Li, D. Liu, Generalized laminate theories based on double superposition hypothesis, Int. J. Numer. Methods Eng. 40 (1997) 1197–1212.

[21] W. Zhen, C. Wanji, A study of global–local higher-order theories for laminated composite plates, Compos. Struct. 79 (2007) 44–54.

[22] A. Catapano, G. Giunta, S. Belouettar, E. Carrera, Static analysis of laminated beams via a unified formulation, Compos. Struct. 94 (2011) 75–83.

[23] A.G. de Miguel, E. Carrera, A. Pagani, E. Zappino, Accurate evaluation of interlaminar stresses in composite laminates via mixed one-dimensional formulation, AIAA J. 56 (2018) 4582–4594.

[24] U. Icardi, A. Urraci, Novel HW mixed zig-zag theory accounting for transverse normal deformability and lower-order counterparts assessed by old and new elastostatic benchmarks, Aerosp. Sci. Technol. 80 (2018) 541–571.

[25] S. Brischetto, E. Carrera, L. Demasi, Improved response of asymmetrically laminated sandwich plates by using zig-zag functions, J. Sandw. Struct. Mater. 11 (2009) 257–267.

[26] U. Icardi, F. Sola, Development of an efficient zig-zag model with variable representation of displacements across the thickness, J. Eng. Mech. 140 (2014) 531–541.

[27] M. Gherlone, On the use of zigzag functions in equivalent single layer theories for laminated composite and sandwich beams: a comparative study and some observations on external weak layers, J. Appl. Mech. 80 (6) (2013) 1–19.

[28] R.M. Groh Jr, P.M. Weaver, On displacement-based and mixed-variational equivalent single layer theories for modeling highly heterogeneous laminated beams, Int. J. Solids Struct. 59 (2015) 147–170.

[29] U. Icardi, A. Urraci, Free and forced vibration of laminated and sandwich plates by zig-zag theories differently accounting for transverse shear and normal deformability, Aerospace 5 (4) (2018) 108.

[30] W. Zhen, C. Wanji, A global higher-order zig-zag model in terms of the HW variational theorem for multi-layered composite beams, Compos. Struct. 158 (2016) 128–136.

[31] H. Matsunaga, Interlaminar stress analysis of laminated composite beams according to global higher-order deformation theories, Compos. Struct. 55 (2002) 105–114.

[32] K. Surana, S. Nguyen, Two-dimensional curved beam element with higher order hierarchical transverse approximation for laminated composites, Comput. Struct. 36 (1990) 499–511.

[33] M.K. Rao, Y. Desai, M. Chistnis, Free vibrations of laminated beams using mixed theory, Compos. Struct. 52 (2001) 149–160.

[34] L. Jun, H. Hongxing, Dynamic stiffness analysis of laminated composite beams using trigonometric shear deformation theory, Compos. Struct. 89 (2009) 433–442.

[35] P. Vidal, O. Polit, Assessment of the refined sinus model for the non-linear analysis of composite beams, Compos. Struct. 87 (2009) 370–381.

[36] M. Karama, K. Afaq, S. Mistou, Mechanical behaviour of laminated composite beam by the new multi-layered laminated composite structures model with transverse shear stress continuity, Int. J. Solids Struct. 40 (2003) 1525–1546.

[37] J. Mantari, A. Oktem, C.G. Soares, A new higher order shear deformation theory for sandwich and composite laminated plates, Composites, Part B, Eng. 43 (2012) 1489–1499.

[38] T.S. Plagianakos, E.G. Papadopoulos, Low-energy impact response of composite and sandwich composite plates with piezoelectric sensory layers, Int. J. Solids Struct. 51 (2014) 2713–2727, https://doi.org/10.1016/j.ijsolstr.2014.04.005.

[39] C.S. Rekatsinas, D.A. Saravanos, A Hermite spline layerwise time domain spectral finite element for guided wave prediction in laminated composite and sandwich plates, J. Vib. Acoust. 139 (2017), https://doi.org/10.1115/1.4035702.

[40] J.-S. Kim, M. Cho, Enhanced first-order theory based on mixed formulation and transverse normal effect, Int. J. Solids Struct. 44 (2007) 1256–1276.

[41] A. Tessler, M. Di Sciuva, M. Gherlone, A refined zigzag beam theory for composite and sandwich beams, J. Compos. Mater. 43 (2009) 1051–1081.

[42] A. Barut, E. Madenci, A. Tessler, A refined zigzag theory for laminated composite and sandwich plates incorporating thickness stretch deformation, in: Proc. 53rd AIAA/ASME/ASCE/AHS/ACS Structures, Structural Dynamics and Materials Conference, Hawaii, 2012.

[43] L. Iurlaro, M. Gherlone, M. Di Sciuva, The (3, 2)-mixed refined zigzag theory for generally laminated beams: theoretical development and C° finite element formulation, Int. J. Solids Struct. 73–74 (2015) 1–19.

[44] M. Shariyat, A generalized global-local higher order theory for bending and vibration analyses of sandwich plates subjected to thermo-mechanical loads, Int. J. Mech. Sci. 52 (2010) 495–514.

[45] E. Carrera, A. Ciuffreda, Bending of composites and sandwich plates subjected to localized lateral loadings: a comparison of various theories, Compos. Struct. 68 (2005) 185–202.

[46] C.S. Rekatsinas, C.V. Nastos, T.C. Theodosiou, D.A. Saravanos, A time-domain high-order spectral finite element for the simulation of symmetric and anti-symmetric guided waves in laminated composite strips, Wave Motion 53 (2015) 1–19.

[47] O. Mattei, L. Bardella, A structural model for plane sandwich beams including transverse core deformability and arbitrary boundary conditions, Eur. J. Mech. A, Solids 58 (2016) 172–186.

[48] U. Icardi, A. Urraci, Free vibration of flexible soft-core sandwiches according to layerwise theories differently accounting for the transverse normal deformability, Lat. Am. J. Solids Struct. 16 (8) (2019) 1–35.

[49] U. Icardi, F. Sola, C° fixed degrees of freedom zigzag model with variable in-plane and out-of plane kinematics and quadrilateral plate element, J. Aerosp. Eng. 28 (2014) 040141351.

[50] U. Icardi, A. Atzori, Simple, efficient mixed solid element for accurate analysis of local effects in laminated and sandwich composites, Adv. Eng. Softw. 35 (2004) 843–859.

[51] W. Zhen, M. Rui, C. Wanji, A C0 three-node triangular element based on preprocessing approach for thick sandwich plates, J. Sandw. Struct. Mater. 00 (2017) 1–23.

[52] W. Zhen, C. Wanji, An efficient higher-order theory and finite element for laminated plates subjected to thermal loading, Compos. Struct. 73 (2006) 99–109.

[53] R.C. Averill, Y.C. Yip, Development of simple, robust finite elements based on refined theories for thick laminated beams, Comput. Struct. 59 (1996) 529–546.